Topics in Molecular Photophysics and Spectroscopy

Martin Vacha

Advanced Course of Soft Material Physics
Advanced Course of Organic Materials for Photonics

Contents

1. Quantum mechanics of the molecule-radiation interaction

Classical treatment of the interaction between an atom or molecule and electromagnetic radiation based on Lorentz oscillator model assumes that an electron is attached to the nucleus by a spring and responds to the oscillating electric field of light. The model correctly predicts the dispersion relation for the real part of the refractive index. To account for the effects of light absorption by atoms or molecules, the model has to rely on introducing an arbitrary damping of the electron oscillatory motion. The damping does not have any apparent physical interpretation in the classical theory. Still, the theory succeeds in correctly predicting the frequency dependence of the imaginary part of the refractive index in the form of the Lorentzian absorption line shape. For the physical meaning of the absorption process we have to turn to the quantum-mechanical description of the molecule-radiation interaction. In the semi-classical approach which will be introduced here the molecule is treated quantum mechanically and its equation of motion is the time-dependent Schrödinger equation. The electromagnetic radiation is treated classically based on Maxwell's equations. This approach is sufficient for the explanation of the processes of light absorption and stimulated emission; the phenomenon of spontaneous emission has to be introduced as phenomenological. For the full treatment of spontaneous emission, theory including quantization of the electromagnetic field would be necessary.

1.1. Unperturbed system

The semi-classical treatment of the molecule-radiation interaction begins with the description of the unperturbed system. Let $\Psi(r,t)$ be the time dependent wavefunction of the molecule. The Schrödinger equation is

$$i\hbar\frac{\partial\Psi(r,t)}{\partial t} = H\Psi(r,t) \qquad (1)$$

where H is the Hamiltonian containing the operators for kinetic and potential energy. If H is time-independent, $\Psi(r,t)$ can be written as a product of space- and time-dependent components

$$\Psi(r,t) = \psi(r)\varphi(t) \qquad (2)$$

States that can be described by Eq. (2) are called stationary states. Inserting (2) into Eq. (1) gives

$$i\hbar\frac{\partial\varphi(t)}{\partial t}\frac{1}{\varphi(t)}=\frac{H\psi(r)}{\psi(r)} \tag{3}$$

For Eq. (3) to be valid for all r and t, both sides must be equal to a constant E. The resulting two equations are

$$H\psi(r)=E\psi(r) \tag{4}$$

which is the time-independent Schrödinger equation for energy eigenvalues, and

$$\frac{\partial\varphi(t)}{\partial t}\frac{1}{\varphi(t)}=-i\frac{E}{\hbar} \tag{5}$$

Eq. (5) is easily solved to give

$$\varphi(t)=\exp(-i\frac{E}{\hbar}t) \tag{6}$$

Thus, the total wavefunction of the unperturbed system is generally

$$\Psi(r,t)=\psi(r)\exp(-i\frac{E}{\hbar}t) \tag{7}$$

Since we are concerned with interaction of the molecule with electromagnetic radiation, we consider, for simplicity, two electron energy states 1 and 2.

state 2 ——————— E_2 $\qquad \Psi_2(r,t)=\psi_2(r)\exp(-i\frac{E_2}{\hbar}t)$

state 1 ——————— E_1 $\qquad \Psi_1(r,t)=\psi_1(r)\exp(-i\frac{E_1}{\hbar}t)$

The corresponding wavefunctions $\Psi_1(r,t)$, $\Psi_2(r,t)$ satisfy the energy eigenvalue equations

$$H\Psi_1(r,t)=E_1\Psi_1(r,t)$$

$$H\Psi_2(r,t)=E_2\Psi_2(r,t) \tag{8}$$

and the time-dependent wavefunctions can be written as

$$\Psi_1(r,t) = \psi_1(r)\exp(-i\frac{E_1}{\hbar}t) \qquad \Psi_2(r,t) = \psi_2(r)\exp(-i\frac{E_2}{\hbar}t) \tag{9}$$

The energy difference between the states corresponds to the transition frequency ω_0:

$$E_2 - E_1 = \hbar\omega_0 \tag{10}$$

The total wavefunction can be written as a linear combination of the wavefunctions of the states 1, 2:

$$\Psi(r,t) = C_1(t)\Psi_1(r,t) + C_2\Psi_2(r,t) \tag{11}$$

which should be normalized at all times

$$\int_V \Psi^*(r,t)\Psi(r,t)dr = \left|C_1(t)\right|^2 + \left|C_2(t)\right|^2 = 1 \tag{12}$$

1.2. Interaction with radiation

Interaction of the molecule with electromagnetic radiation results in change of the molecular potential energy which can be described by introducing a new Hamiltonian

$$H + H'$$

where H is the unperturbed part from Eq. (8) and H' is the interaction part. The corresponding Schrödinger equation can be written as

$$i\hbar\frac{\partial}{\partial t}\left(C_1(t)\Psi_1(r,t) + C_2(t)\Psi_2(r,t)\right) = (H + H')\left(C_1(t)\Psi_1(r,t) + C_2(t)\Psi_2(r,t)\right) \tag{13}$$

Given the known stationary solutions of the unperturbed states in the form

$$i\hbar\frac{\partial\Psi_i(r,t)}{\partial t} = H\Psi_i(r,t) \tag{14}$$

the Eq. (13) gives

$$i\hbar\left(\Psi_1\frac{dC_1}{dt} + \Psi_2\frac{dC_2}{dt}\right) = H'\left(C_1\Psi_1 + C_2\Psi_2\right) \tag{15}$$

where the space and time dependence notation has been omitted for simplicity. Multiplying Eq. (15) from left by Ψ_1^*, integrating over all space and making use of the

normalization and orthogonality conditions gives on the left side

$$i\hbar\left(\int \Psi_1^* \Psi_1 dr \frac{dC_1}{dt} + \int \Psi_1^* \Psi_2 dr \frac{dC_2}{dt}\right) = i\hbar \frac{dC_1}{dt} \tag{16}$$

and on the right side

$$C_1 \int \psi_1^* \exp(i\frac{E_1}{\hbar}t) H' \psi_1 \exp(-i\frac{E_1}{\hbar}t) dr + C_2 \int \psi_1^* \exp(i\frac{E_1}{\hbar}t) H' \psi_2 \exp(-i\frac{E_2}{\hbar}t) dr \tag{17}$$

Combining (16) and (17), we obtain

$$i\hbar \frac{dC_1}{dt} = C_1 \int \psi_1^* H' \psi_1 dr + C_2 \exp(-i\omega_0 t) \int \psi_1^* H' \psi_2 dr \tag{18}$$

and similarly

$$i\hbar \frac{dC_2}{dt} = C_2 \int \psi_2^* H' \psi_2 dr + C_1 \exp(i\omega_0 t) \int \psi_2^* H' \psi_1 dr \tag{19}$$

The Eqs. (18) and (19) are time dependent Schrödinger equations for the coefficients C_1 and C_2 which can be, in principle, solved for any given form of the interaction Hamiltonian *H'*.

1.3. Form of the interaction Hamiltonian for harmonic perturbation

Electromagnetic radiation is usually described by oscillating electric field characterized by frequency ω and propagation number *k*:

$$E = E_0 \cos(kz - \omega t) \tag{20}$$

For optical frequencies, the size of typical molecule is much smaller than the wavelength and spatial variations of electric field across the molecule are negligible. We may therefore drop the space dependence of electric field and use

$$E = E_0 \cos(\omega t) \tag{21}$$

Considering a molecule, the electric field will act upon a dipole moment

$$\boldsymbol{\mu} = -e\sum_i \mathbf{r}_i = -e\mathbf{r} \tag{22}$$

where the sum is over all electrons contributing to the dipole moment and *e* is electron

charge. Due to the interaction the corresponding potential energy will be changed by $\mathbf{E}\cdot\boldsymbol{\mu}$. Assuming for simplicity that $\mathbf{E}$ points in the x direction, the corresponding interaction Hamiltonian is written as

$$H' = E_0\cos(\omega t)|\mu| = eE_0\cos(\omega t)x \tag{23}$$

where x is the x-component of $\mathbf{r}$. The operator H' has an odd parity $H'(-r) = -H'(r)$, meaning that $\psi_i^* H'\psi_i$ must also have odd parity and

$$\int \psi_1^* H'\psi_1 dr = 0 \quad \text{and} \quad \int \psi_2^* H'\psi_2 dr = 0$$

The Schrödinger equations for coefficients C_1 and C_2 then simplify to

$$i\hbar\frac{dC_1}{dt} = C_2\exp(-i\omega_0 t)E_0\cos(\omega t)|\mu_{21}|$$

$$i\hbar\frac{dC_2}{dt} = C_1\exp(i\omega_0 t)E_0\cos(\omega t)|\mu_{12}| \tag{24}$$

where the dipole moment matrix elements are

$$|\mu_{21}| = e\int \psi_1^* x\psi_2 dr \quad \text{and} \quad |\mu_{12}| = e\int \psi_2^* x\psi_1 dr \tag{25}$$

The matrix elements given in Eq. (25) describe electric dipole moments due to transitions between states 1 and 2, and as such are called *transition dipole moments* of electronic transitions.

1.4. Approximate solutions: perturbation theory

General solutions of the Schrödinger equations (24) are complicated and the equations are often solved approximately using time-dependent perturbation theory. Perturbation theory can be applied in cases where the Hamiltonian is in the form $H+H'$, H representing Hamiltonian of the unperturbed system and H' the perturbation. If the solutions (wavefunctions and energies) of the unperturbed system are known exactly and if the perturbation H' is small compared to H, the solutions of the perturbed system can be found using the unperturbed solutions as a basis. In the case of Eqs. (24) we

assume that the perturbation E_0 is small compared to the energy of the system, and we may set the initial values at time $t = 0$ to $C_1(0) = 1$ and $C_2(0) = 0$. This initial condition states that the molecule is in state 1 (called *ground state*) at $t = 0$. Solving the Eqs. (24) for these initial values will give solutions in the first order of perturbation theory which, for our purpose, will be sufficient. Using the first order solution in the Eqs. (24) would further give solutions in the second order, and repetition of this process would result in an approximate solution that could be written as a power series of E_0, describing *nonlinear* optical effects.

Using $C_1(0) = 1$ and $C_2(0) = 0$ in Eq. (24) gives

$$i\hbar \frac{dC_1}{dt} = 0 \tag{26}$$

which has a trivial solution, and

$$i\hbar \frac{dC_2}{dt} = E_0 |\mu_{12}| \exp(i\omega_0 t)\cos(\omega t) \tag{27}$$

Using the identity $2\cos(\omega t) = \exp(i\omega t) + \exp(-i\omega t)$ we obtain

$$\frac{dC_2}{dt} = -i\frac{E_0|\mu_{12}|}{\hbar}\frac{1}{2}\left(\exp(i(\omega_0 + \omega)t) + \exp(i(\omega_0 - \omega)t)\right) \tag{28}$$

The Eq. (28) should now be integrated with respect to time from 0 to t, which is the period for which the perturbation acts upon the system.

Using $\int \exp(ax)dx = 1/a \exp(ax) + c$ we obtain, for example

$$\int_0^t \exp(i(\omega_0 + \omega)t)dt = \frac{\exp(i(\omega_0 + \omega)t) - 1}{i(\omega_0 + \omega)}$$

and the solution for C_2(t) in the first order of perturbation theory as

$$C_2(t) = \frac{E_0|\mu_{12}|}{\hbar}\frac{1}{2}\left(\frac{1 - \exp(i(\omega_0 + \omega)t)}{\omega_0 + \omega} + \frac{1 - \exp(i(\omega_0 - \omega)t)}{\omega_0 - \omega}\right) \tag{29}$$

Taking into account the magnitude of electromagnetic frequencies near resonance ω_0, $\omega_0 + \omega >> \omega_0 - \omega$ and we may neglect the first term in Eq. (29). This approximation is usually called *rotating wave* approximation. The Eq. (29) then simplifies to

$$C_2(t) = \frac{E_0|\mu_{12}|}{\hbar}\frac{1}{2}\left(\frac{1-\exp(i(\omega_0-\omega)t)}{\omega_0-\omega}\right) \tag{30}$$

Instead of the value of coefficient C_2(t) we will calculate the physically important quantity $C_2^*(t)C_2(t) = |C_2(t)|^2$ which gives the probability that the molecule will be in state 2 (*excited* state) at time *t*.

$$|C_2(t)|^2 = \frac{E_0^2|\mu_{12}|^2}{\hbar^2}\frac{1}{4}\left(\frac{2-\exp(-i(\omega_0-\omega)t)-\exp(i(\omega_0-\omega)t)}{(\omega_0-\omega)^2}\right) \tag{31}$$

Using $\cos\alpha = \cos^2\alpha/2 - \sin^2\alpha/2$ the solution simplifies to

$$|C_2(t)|^2 = \frac{E_0^2|\mu_{12}|^2}{\hbar^2}\left(\frac{\sin^2\left(\frac{\omega_0-\omega}{2}t\right)}{(\omega_0-\omega)^2}\right) \tag{32}$$

The requirement that E_0 be small ensures that the approximate solution (32) does not violate the normalization condition.

The solution (32) is plotted in Figure 1 as a function of the detuning $\omega_0 - \omega$. As expected, the probability of finding the molecule in excited state is maximum for $\omega_0 = \omega$, where it is proportional to t^2. However, if the time *t* is finite, the probability is non-zero for certain values of $\omega_0 - \omega$, a fact that is related to the Heisenberg uncertainty principle.

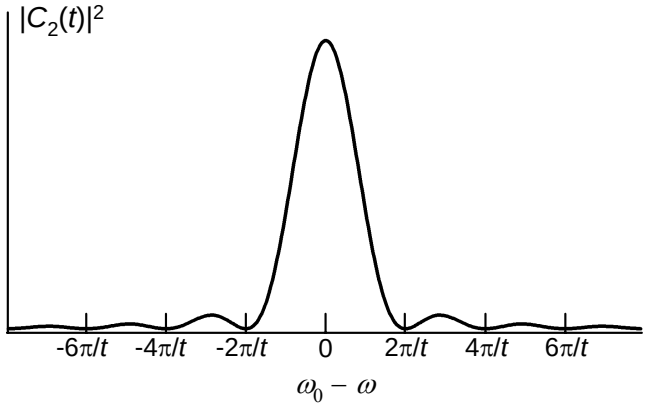

Figure 1

1.5. Transition rate

Another important physical quantity is the transition rate between states 1 and 2, which gives rate of the absorption of light by the molecule (number of photons absorbed per second). The rate is defined as the probability of finding the molecule in the excited state divided by time *t*

$$\Gamma_{12} = \frac{|C_2(t)|^2}{t} = \frac{E_0^2|\mu_{12}|^2}{4\hbar^2}\left(\frac{\sin^2\left(\frac{\omega_0-\omega}{2}t\right)}{\left(\frac{\omega_0-\omega}{2}\right)^2 t}\right) \tag{33}$$

The time-dependence in (33) can be eliminated by using the limit

$$\lim_{t\to\infty}\frac{\sin^2(at)}{a^2 t} = 2\pi\delta(a)$$

where $\delta(a)$ is Dirac's delta function. The expression (33) simplifies to

$$\Gamma_{12} = \frac{\pi}{2\hbar^2}E_0^2|\mu_{12}|^2\delta(\omega_0-\omega) \tag{34}$$

which is an important result in quantum mechanics, often referred to as *Fermi' golden rule*. In its general from, Fermi's golden rule states that the probability of a quantum-mechanical transition is proportional to the square of the matrix element of the interaction Hamiltonian.

Instead of the electric field amplitude E_0 which does not take into account the frequency dependence we may use the electromagnetic field energy density defined as

$$\int W(\omega)d\omega = \tfrac{1}{2}\varepsilon_0 E_0^2 \tag{35}$$

and use well-known property of the Dirac's delta function

$$\int W(\omega)d\omega\delta(\omega_0-\omega) = W(\omega_0) \tag{36}$$

to obtain

$$\Gamma_{12} = \frac{\pi}{\varepsilon_0\hbar^2}|\mu_{12}|^2 W(\omega_0) \tag{37}$$

The transition rate is related to the Einstein's coefficient of absorption B_{12} via

$\Gamma_{12} = B_{12}W(\omega_0)$. The expression (37) was derived for the *x*-component of the dipole moment. From averaging over all orientations a correction factor of 1/3 has to be added in the Eq. (37). The resulting expression for the Einstein's coefficient B_{12} thus reads

$$B_{12} = \frac{\pi}{3\varepsilon_0\hbar^2}\left|\mu_{12}\right|^2 \tag{38}$$

The expression for the Einstein' coefficient of stimulated emission B_{21} could be obtained in the same way by taking $E_2 - E_1 = -\hbar\omega_0$ in Eq. (10). One would obtain $B_{12} = B_{21}$.

1.6. Spontaneous emission

The treatment presented so far describes processes of absorption and stimulated emission – processes that occur *only* in the presence of the perturbation. As seen from the Fermi's golden rule (37), if $W(\omega_0) = 0$ (without light) the rate $\Gamma_{12} = 0$ and the transition does not occur. After the perturbation is switched off, molecule in the excited state would stay in this state forever. This is contrary to the experimental observation that molecules decay to their ground states *spontaneously* in relatively short times. The corresponding process is called spontaneous emission. For full treatment of spontaneous emission it is necessary to use quantum theory of electromagnetic field. In semi-classical approach, the effect of spontaneous emission can introduced phenomenologically into the Schrödinger equation for coefficient C_2 (24) as a new decay route.

$$\frac{dC_2}{dt} = -iC_1\frac{E_0\left|\mu_{12}\right|}{\hbar}\exp(i\omega_0 t)\cos(\omega t) - \gamma_{SP}C_2 \tag{39}$$

In the absence of perturbation ($E_0 = 0$)

$$\frac{dC_2}{dt} = -\gamma_{SP}C_2 \tag{40}$$

which is solved easily to obtain

$$C_2(t) = C_2(0)\exp(-\gamma_{SP}t) \tag{41}$$

In (41), the phenomenological constant γ_{SP} is related to the Einstein's coefficient A as $2\gamma_{SP} = A$, and to the excited state radiative lifetime τ_R as

$$\frac{1}{\tau_R} = 2\gamma_{SP} \tag{42}$$

For completeness, the Einstein's coefficients for stimulated and spontaneous processes are related as

$$A = \frac{\hbar\omega^3}{\pi^2 c^3} B_{12} \tag{43}$$

The processes of absorption, stimulated emission and spontaneous emission are shown symbolically in Figure 2.

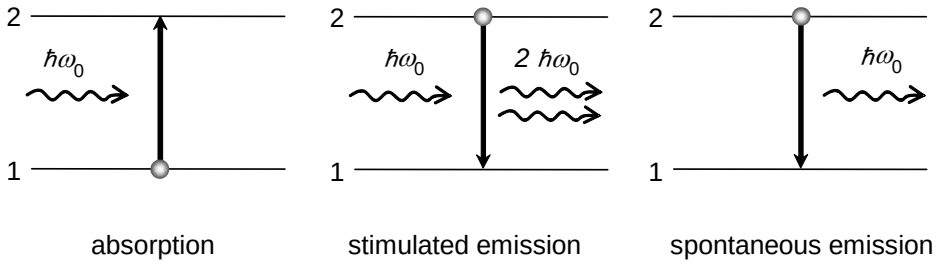

Figure 2

1.7. General solutions: optical Bloch equations

The Eqs. (24) provide an exact description of the state of two-level molecule in the presence of oscillating electric field. The solutions by perturbation theory are approximations in the sense that they retain only first order solutions for very weak perturbation. For more general description, it is useful to introduce density matrix ρ_{ij} defined as

$$\rho_{11} = |C_1|^2 \qquad \rho_{22} = |C_2|^2$$

$$\rho_{12} = C_1 C_2^* \qquad \rho_{21} = C_2 C_1^* \tag{44}$$

The diagonal elements represent populations of the ground and excited states while the off-diagonal elements describe *coherences*, that is relationship between phases of the two state wavefunctions. The definition (44) leads to the following conditions

$$\rho_{11} + \rho_{22} = 1 \quad \text{(normalization)} \qquad \rho_{12} = \rho_{21}^* \tag{45}$$

Equations of motion for the density matrix are expressed as

$$\frac{d\rho_{ij}}{dt} = C_i \frac{dC_j^*}{dt} + C_j^* \frac{dC_i}{dt} \tag{46}$$

The derivations with respect to time of coefficients C_i can be taken from the Eqs. (24). Substitution of (24) to (46) yields

$$\frac{d\rho_{22}}{dt} = -i\Omega_R \cos(\omega t)\left(\rho_{12}\exp(i\omega_0 t) - \rho_{21}\exp(-i\omega_0 t)\right) \tag{47}$$

where we used the symbol Ω_R for

$$\Omega_R = \frac{E_0|\mu_{12}|}{\hbar} \tag{48}$$

Similarly,

$$\frac{d\rho_{11}}{dt} = -\frac{d\rho_{22}}{dt} \tag{49}$$

and

$$\frac{d\rho_{12}}{dt} = i\Omega_R \cos(\omega t)\exp(-i\omega_0 t)\left(\rho_{11} - \rho_{22}\right) \tag{50}$$

Using again $2\cos(\omega t) = \exp(i\omega t) + \exp(-i\omega t)$ and the rotating frame approximation, that is neglecting the fast oscillating terms $\exp(i(\omega_0 + \omega)t)$, we can rewrite (47) as

$$\frac{d\rho_{22}}{dt} = -i\frac{\Omega_R}{2}\left(\rho_{12}\exp(i(\omega_0 - \omega)t) - \rho_{21}\exp(-i(\omega_0 - \omega)t)\right) \tag{51}$$

By using a substitution

$$\tilde{\rho}_{12} = \exp(i(\omega_0 - \omega)t)\rho_{12} \qquad \tilde{\rho}_{21} = \exp(-i(\omega_0 - \omega)t)\rho_{21}$$

$$\tilde{\rho}_{11} = \rho_{11} \qquad \tilde{\rho}_{22} = \rho_{22} \tag{52}$$

the Eqs. (47), (49) and (50) become

$$\frac{d\tilde{\rho}_{22}}{dt} = -\frac{d\tilde{\rho}_{11}}{dt} = -i\frac{\Omega_R}{2}\left(\tilde{\rho}_{12} - \tilde{\rho}_{21}\right) \tag{53}$$

$$\frac{d\tilde{\rho}_{12}}{dt} = -\frac{d\tilde{\rho}_{21}^*}{dt} = -i\frac{\Omega_R}{2}\left(\tilde{\rho}_{11} - \tilde{\rho}_{22}\right) + i(\omega_0 - \omega)\tilde{\rho}_{12} \tag{54}$$

The set of equations (53) and (54) is known as *optical Bloch* equations describing the interaction of 2-level molecule with classical electromagnetic radiation. When solving the set of first order differential equations we assume the solution in the form

$$\tilde{\rho}_{ij}(t) = \tilde{\rho}_{ij}(0)\exp(\lambda t) \tag{55}$$

and insert the assumed solution into Eqs. (53) and (54). For the Eq. (53), for example, we obtain

$$-\lambda\tilde{\rho}_{22}(0) - i\frac{\Omega_R}{2}\tilde{\rho}_{12}(0) + i\frac{\Omega_R}{2}\tilde{\rho}_{21}(0) = 0$$

Combining with expressions obtained from the other equations we may write a matrix form

$$\begin{pmatrix} -\lambda & 0 & i\frac{\Omega_R}{2} & -i\frac{\Omega_R}{2} \\ 0 & -\lambda & -i\frac{\Omega_R}{2} & i\frac{\Omega_R}{2} \\ i\frac{\Omega_R}{2} & -i\frac{\Omega_R}{2} & i(\omega_0-\omega)-\lambda & 0 \\ -i\frac{\Omega_R}{2} & i\frac{\Omega_R}{2} & 0 & -i(\omega_0-\omega)-\lambda \end{pmatrix} \begin{pmatrix} \tilde{\rho}_{11}(0) \\ \tilde{\rho}_{22}(0) \\ \tilde{\rho}_{12}(0) \\ \tilde{\rho}_{21}(0) \end{pmatrix} = 0 \tag{56}$$

The condition that the determinant of the above 4x4 matrix is equal to 0 gives the equation for the coefficients λ

$$\lambda^2\left(\lambda^2 + (\omega_0-\omega)^2 + \Omega_R^2\right) = 0 \tag{57}$$

The equation (57) has three roots

$$\lambda_1 = 0 \quad \text{and} \quad \lambda_{2,3} = \pm i\sqrt{(\omega_0-\omega)^2 + \Omega_R^2} = \pm i\Omega \tag{58}$$

where we have introduced a new symbol Ω for simplicity. Using the three roots (58) we can write the general solution of Bloch equations in the form

$$\tilde{\rho}_{ij}(t) = \tilde{\rho}_{ij}^{(1)} + \tilde{\rho}_{ij}^{(2)}\exp(i\Omega t) + \tilde{\rho}_{ij}^{(3)}\exp(-i\Omega t) \tag{59}$$

The three coefficients $\tilde{\rho}_{ij}^{(1)}, \tilde{\rho}_{ij}^{(2)}, \tilde{\rho}_{ij}^{(3)}$ can be determined from the initial values $\tilde{\rho}_{ij}(0)$

for a given problem and from the first and second derivatives at time $t = 0$ of the matrix elements obtained from the Bloch equations, $\left[\frac{d\tilde{\rho}_{ij}(t)}{dt}\right]_{t=0}$ and $\left[\frac{d^2\tilde{\rho}_{ij}(t)}{dt^2}\right]_{t=0}$. For the initial conditions of the molecule being in the ground state,

$$\tilde{\rho}_{22}(0) = 0 \quad , \quad \tilde{\rho}_{11}(0) = 1 \quad \text{and} \quad \tilde{\rho}_{12}(0) = \tilde{\rho}_{21}(0) = 0 \tag{60}$$

solving the respective three equations for the $\tilde{\rho}_{ij}^{(1)}, \tilde{\rho}_{ij}^{(2)}, \tilde{\rho}_{ij}^{(3)}$ coefficients gives

$$\tilde{\rho}_{22}(t) = \frac{\Omega_R}{\Omega}\sin^2\left(\frac{\Omega t}{2}\right) \tag{61}$$

For the case of resonance $\omega_0 = \omega$, the definition (58) gives $\Omega_R = \Omega$ and (61) further simplifies to

$$\tilde{\rho}_{22}(t) = \sin^2\left(\frac{\Omega_R t}{2}\right) \tag{62}$$

As can be seen from Eq. (62), the population *oscillates* periodically between ground and excited states with frequency Ω_R. This phenomenon occurring during the interaction of a two-level molecule with strong electromagnetic field is called Rabi oscillation and the corresponding frequency Ω_R is a *Rabi frequency*. Figure 3 shows the Rabi oscillations for various values of the detuning ($\omega_0 - \omega$).

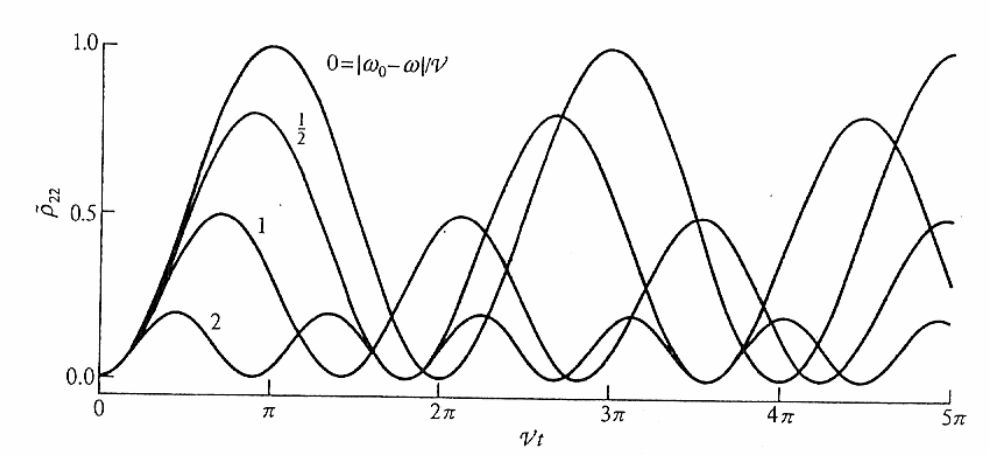

Figure 3 (reprinted from [1])

1.8. Effect of spontaneous emission in Bloch equations

The effect of spontaneous emission can be included in Bloch equations phenomenologically, similar to Eq. (39). The resulting equations have the form

$$\frac{d\tilde{\rho}_{22}}{dt} = -\frac{d\tilde{\rho}_{11}}{dt} = -i\frac{\Omega_R}{2}\left(\tilde{\rho}_{12} - \tilde{\rho}_{21}\right) - 2\gamma_{SP}\tilde{\rho}_{22} \tag{63}$$

$$\frac{d\tilde{\rho}_{12}}{dt} = -\frac{d\tilde{\rho}_{21}^{*}}{dt} = -i\frac{\Omega_R}{2}\left(\tilde{\rho}_{11} - \tilde{\rho}_{22}\right) + \left(i(\omega_0 - \omega) - \gamma_{SP}\right)\tilde{\rho}_{12} \tag{64}$$

The solution of the equations (63) and (64) proceeds in a similar way as that of the Eqs. (53) and (54) by solving the roots of a 4x4 matrix determinant. For the initial conditions (60) the solution for the excited state population is

$$\tilde{\rho}_{22}(t) = \frac{\Omega_R^2}{2\left(2\gamma_{SP}^2 + \Omega_R^2\right)}\left[1 - \left(\cos(\Lambda t) + \frac{3\gamma_{SP}}{2\Lambda}\sin(\Lambda t)\right)\exp\left(-\frac{3\gamma_{SP}t}{2}\right)\right] \tag{65}$$

where $\Lambda = \sqrt{\Omega_R^2 - \frac{1}{4}\gamma_{SP}^2}$. Figure 4 shows the effect of increasing ratio γ_{SP}/Ω_R on the Rabi oscillatory behavior. Increasing radiative rate γ_{SP} causes increased damping of the Rabi oscillations which disappear completely for $\gamma_{SP}/\Omega_R > 1$.

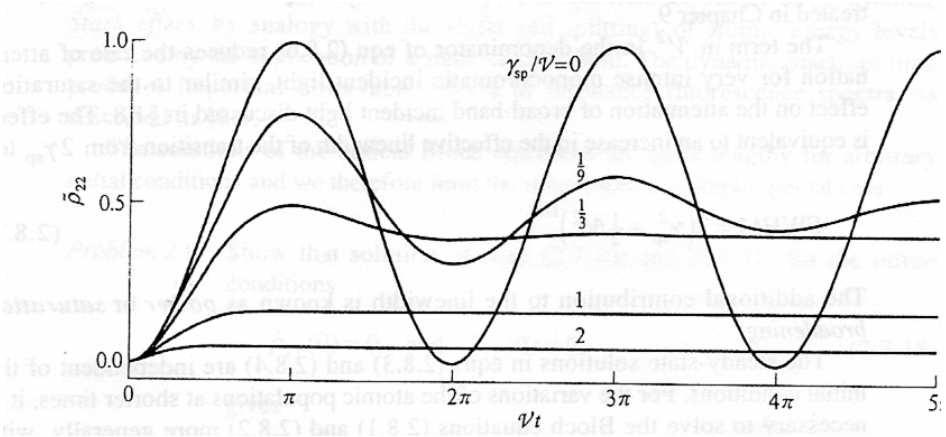

Figure 4 (reprinted from [1])

2. Excited states of organic molecules and excited state relaxations

The preceding chapter dealt with general description of the interaction of light with a quantum mechanical system, described by a wavefunction $\Psi(r,t)$. In this chapter, we will specify the ground and excited states of molecules that correspond to transitions in the optical part of electromagnetic spectrum. We will also deal with the various processes that lead to the formation and relaxation of molecular excited states.

2.1. Classification of excited states

Molecules with electronic excited states and transitions in the UV and visible part of the spectrum can be broadly divided into three groups:

1. Molecules that absorb radiation because of an electronic transition localized on a single bond. An example is a carbonyl group > C = O, which gives rise to absorption of light at about 290 nm.
2. Molecules containing conjugated π-electron systems, where the electrons of C = C bonds become delocalized and are responsible for the molecules' ability to absorb light in the entire visible range due to π–π* transitions.
3. Molecules that contain a transition metal ion in a coordination compound. The interaction of the *d* electrons with the ligands lifts the 5-fold degeneracy and enables transitions between the split *d* orbital levels (*d-d* transitions). Such transitions are often in the visible part of the spectrum.

Of the above categories, the conjugated systems are by far the most important group of molecules with optical electronic transitions and the rest of the talk will concentrate on these systems.

2.2. Electronic states of conjugated and aromatic systems

There are several methods that can be used to calculate the electronic states of conjugated systems. These include MO LCAO, free electron method for linear conjugated systems or perimeter-free electron orbital model for aromatic systems. In the Hückel approximation, the σ and π electrons are treated independently, the latter being considered responsible for the optical properties. As an example, electronic states of the molecule of benzene can be expressed as linear combinations of the six 2pπ orbitals φ_A, φ_B, ... φ_F of individual carbon atoms. The possible linear combinations of the atomic orbitals are restricted by the requirement that the resulting molecular electronic wavefunctions confirm to the symmetry of the molecule. The group theory of molecular

symmetry gives the following six molecular orbitals as linear combinations based on the properties of the D_{6h} symmetry group of benzene as

$$\begin{aligned}
\psi_{a1} &= \varphi_A + \varphi_B + \varphi_C + \varphi_D + \varphi_E + \varphi_F \\
\psi_{b1} &= \varphi_A - \varphi_B + \varphi_C - \varphi_D + \varphi_E - \varphi_F \\
\psi_{e1} &= 2\varphi_A + \varphi_B - \varphi_C - 2\varphi_D - \varphi_E + \varphi_F \\
\psi_{e1} &= \varphi_A + 2\varphi_B + \varphi_C - \varphi_D - 2\varphi_E - \varphi_F \\
\psi_{e2} &= 2\varphi_A - \varphi_B - \varphi_C + 2\varphi_D - \varphi_E - \varphi_F \\
\psi_{e2} &= \varphi_A - 2\varphi_B + \varphi_C + \varphi_D - 2\varphi_E + \varphi_F
\end{aligned} \qquad (1)$$

The symbols *a*, *b*, *e* correspond to the respective symmetries of the states. Graphical depiction of the resulting π molecular orbitals together with the corresponding energies are shown in Figure 5. The lowest *a* state is fully-bonding, the highest *b* state fully anti-bonding, the *e* states are doubly degenerate. The lowest electronic transition occurs from e_{1g} (π) to e_{2u} (π^*). The two shades represent phases of the molecular wavefunctions, pointing either up or down with respect to the plane of the molecule. Apart from the symmetry notation that originates from the character table of the respective symmetry point group, the subscripts *u* and *g* refer to the wavefunction being either even (*g*) or odd (*u*) with respect to reflection in the center of gravity (a property called *parity*).

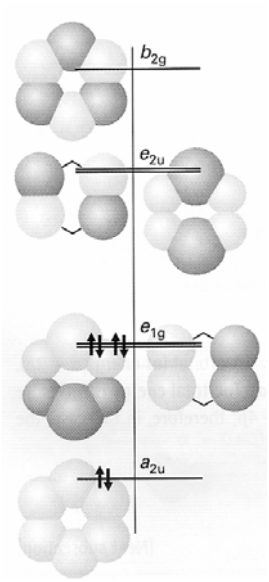

Figure 5
(reprinted from [6])

The six-fold degenerate 2p orbital energy levels of individual atoms split into 6 energy levels of the molecule:

$$E_{1,2} = \alpha \pm 2\beta \qquad E_{3,4} = \alpha \pm \beta \qquad E_{5,6} = \alpha \pm \beta \qquad (2)$$

Two of the energy levels are doubly-degenerate. The symbols α and β correspond to *Coulomb* and *resonance (exchange) integrals*, defined as

$$\alpha = \int \varphi_M^* H \varphi_M dV \qquad \beta = \int \varphi_N^* H \varphi_M dV \qquad (3)$$

where the indices *M*, *N* denote neighboring atomic orbitals and *H* is the interaction Hamiltonian.

The effect of the length of the linear conjugated system or the size of the aromatic system on the electronic wavefunctions and energies can be easily illustrated using the electron-free models. For example, in the perimeter free electron orbital model (PFEO), an electron is considered as moving freely in a one-dimensional loop around the aromatic molecular perimeter. The problem is equal to the problem of a particle in 1-dimensional potential well. Assuming the potential energy at the bottom of the well to be zero and outside of the well infinity, the time-independent Schrödinger equation to be solved has the form

$$-\frac{\hbar^2}{2m}\frac{\partial^2\psi(x)}{\partial x^2} = E\psi(x) \tag{4}$$

The wavefunction must satisfy the boundary condition

$$\psi(x) = \psi(x+l) \tag{5}$$

where x is the coordinate along the perimeter and l is the perimeter length. Solution of the Schrödinger equation gives

$$\begin{aligned} \psi_0 &= \sqrt{1/l} \\ \psi_{n1}(x) &= \sqrt{1/l}\cos(2\pi nx/l) \\ \psi_{n2}(x) &= \sqrt{1/l}\sin(2\pi nx/l) \end{aligned} \tag{6}$$

for the wavefunctions and

$$E_n = \frac{n^2h^2}{2ml^2} \tag{7}$$

for the energy, with m being the electron mass. For the quantum number $n > 0$, each state is doubly degenerate because the electron can move clockwise or anticlockwise around the perimeter. Dependence of the state energy on the perimeter as l^{-2} is now obvious from Eq. (7). With increasing conjugation length, i.e. with increasing number of aromatic rings, the energy of the states, as well as the energy separation between adjacent states, decreases. This decrease gives rise to the well-known optical property of π-conjugated systems, i.e. the spectral red shift with the increase of conjugation length.

2.3. Singlet and triplet states.

So far, we have not included explicitly electron spin in the treatment of the light-molecule interaction. Each energy level can be populated by two electrons with opposite spins (+1/2, -1/2). Upon electronic transition, the electron can either remain in the same spin state, resulting in anti-parallel configuration, or change its spin, resulting in parallel configuration. The anti-parallel (or paired) configuration state, for which the total spin number S = 0, is called *singlet* state. On the other hand, there are three different ways to achieve the parallel configuration (the one for which |S|=1), with the resulting projection of the total spin onto *z*-axis being M_s = -1, 0, 1. As a result, the parallel configuration state is triply degenerate and as such is called a *triplet* state. The situation is schematically shown in Figure 6. It can be shown based on Pauli's principle that two electrons with anti-parallel spins have non-zero probability to be found at the same location, while for parallel-spin electrons this probability is zero. Thus, on average, parallel-spin electrons are farther apart in space and the resulting lower Coulomb repulsion lowers the energy of triplet state with respect to singlet.

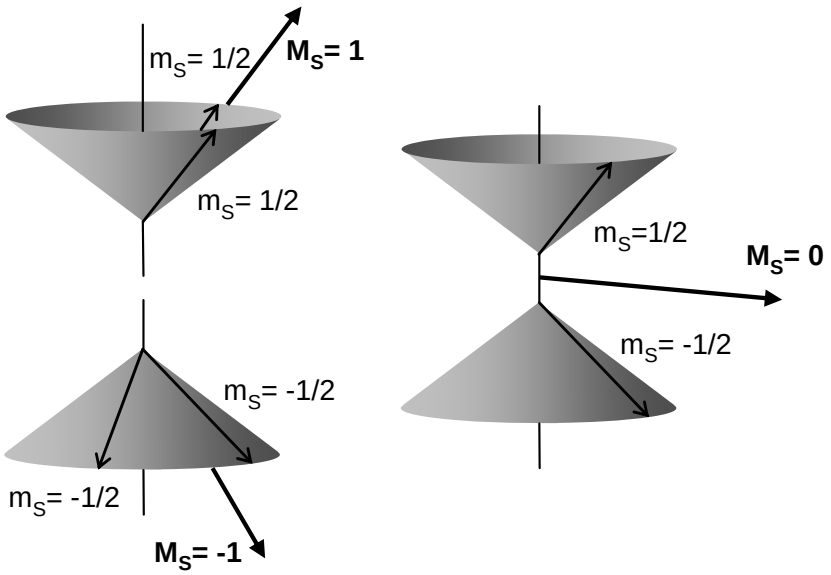

Figure 6

2.4. Basic selection rules

In the previous chapter we have derived an expression for the rate of electronic transition in the form of Fermi's golden rule (Eq. (34)). The expression contains the matrix element of the transition dipole moment

$$\boldsymbol{\mu}_{12} = -e\int \psi_2^* \mathbf{r}\, \psi_1 dr = \int \psi_2^* \boldsymbol{\mu}\, \psi_1 dr \qquad (8)$$

For the transition to have finite probability the integral in Eq. (8) must be non-zero. This condition gives rise to a set of conditions called *selection rules* that the electronic states have to fulfill for the transition to occur. Each electronic state is characterized by a few basic parameters: energy, spin multiplicity, symmetry, and for centrosymmetric molecules also parity. Except of energy, these properties contribute to the value of the integral (8). Basic selection rules are:

1. *Symmetry*. Essentially, electric dipole transitions between electronic states of the same symmetry are forbidden. This selection rule is not obvious by a glance at (8), and the integrand has to be evaluated for each *x*, *y* and *z* component of the vector **r** with respect to the symmetry of individual components. In terms of symmetry group theory, only if the product has the symmetry A_1 will the integral be non-zero. Ground electronic states are generally occupied by paired electrons and as such have the A_1 symmetry. The whole integrand (8) will be of the symmetry type A_1 if both the transition dipole moment operator (any of its *x*, *y*, *z* components) and the excited state wavefunction belong to the same symmetry type.

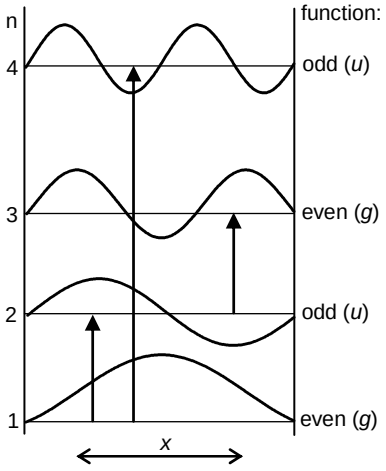

Figure 7

2. *Parity*. In contrast to the symmetry selection rule, the parity selection rule is easy to understand by realizing that the integral (8) vanishes for integrands of odd parity. Since the operator **r** itself has an odd parity, the parity of the states 1 and 2 must be different. Thus, *g* – *u* and *u* – *g* transitions are allowed while *u* – *u* and *g* – *g* transitions are forbidden. This selection rule is illustrated schematically in Figure 7 for wavefunctions of a particle-in-box.
3. *Spin-multiplicity*. To understand this rule, the Eq. (8) has to be re-written using wavefunctions including spin components. The wavefunctions ψ_i will be thus products of the spatial and spin parts

$$\psi_i = \psi_i(r)\chi_i(\sigma) \qquad (9)$$

The Eq. (8) will now have the form

$$\boldsymbol{\mu}_{12} = \int \psi_2^*(r)\chi_2^*(\sigma)\boldsymbol{\mu}\,\psi_1(r)\chi_1(\sigma) dr d\sigma \qquad (10)$$

The transition dipole operator acts only on the spatial part of the wavefunction. The integration in the Eq. (10) can be thus separated according to the coordinates as

$$\boldsymbol{\mu}_{12} = \int \psi_2^*(r)\boldsymbol{\mu}\psi_1(r)dr \int \chi_2^*(\sigma)\chi_1(\sigma)d\sigma \qquad (11)$$

The condition of orthogonality of the spin wavefunctions means that the second integral in the Eq. (11) can be non-zero only when $\chi_2(\sigma) = \chi_1(\sigma)$, i.e. when the spin states of the ground and excited states are same. In other words, the spin multiplicity rule states that electric dipole transitions between states of different spin multiplicity are forbidden. In conjugated systems, spin multiplicity refers to either singlet (non-degenerate state) or to triplet (triple-degenerate state).

2.5. Overview of uni-molecular photophysical processes

The Chapter 1 dealt with theoretical treatment of absorption, stimulated and spontaneous emission. The three phenomena are basis of complex photophysical processes that can occur on an isolated molecule upon interaction with light. In describing the processes, it is customary in literature to use the following notation:

- S_0 ground singlet state (state 1 of the preceding chapter)
- S_1 first excited singlet state (state 2 of the preceding chapter)
- S_n higher excited singlet states (n>1)
- T_1 first excited triplet state
- T_n higher excited triplet states (n>1)

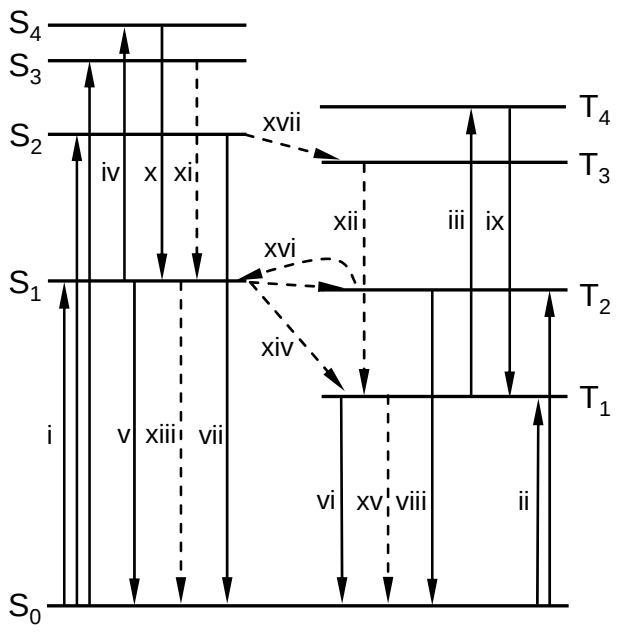

It should be noted that, by definition, the ground state corresponding to T_1 is S_0, i.e., ground triplet state T_0 does not exist. The processes can be illustrated by the so called *Jablonski* diagram (Figure 8), in which energy levels are drawn as horizontal lines, upward pointing arrows correspond to population of higher states and downward

Figure 8

arrows to depopulation (relaxation) of excited states. The full lines depict processes in which light takes part (radiative), the broken lines processes without involvement of light (radiationless). The photophysical processes can be divided into the following categories:

a) *Absorption (radiative excitation) transitions*. Spin-allowed $S_0 - S_1$ and $S_0 - S_n$ are the most often encountered transitions (i). $S_0 - T_1$ and $S_0 - T_n$ are spin-forbidden but can be observed using strong light sources (ii). $T_1 - T_n$ are spin-allowed and are commonly observed using pulsed excitation (iii). $S_1 - S_n$ can be observed using short pulse excitation (iv).

b) *Luminescence (emission or radiative de-excitation) processes.* Transitions between states of the same multiplicity are called *fluorescence*, those between states of different multiplicity *phosphorescence*. $S_1 - S_0$ fluorescence is most commonly observed luminescence process, occurring on ns time scales (v). $T_1 - S_0$ phosphorescence is spin-forbidden, resulting in weak, long-lifetime process (vi). $S_n - S_0$ fluorescence is a rare process observed in only a few compounds (azulene) (vii). $T_n - S_0$ phosphorescence is also a rare process, observed e.g. in fluoranthene (viii). $T_n - T_1$ fluorescence is an allowed process observed, e.g., in azulene (ix).

c) *Radiationless transitions.* Transitions between states of the same multiplicity are called *internal conversion*, those between states of different multiplicity *intersystem crossing*. $S_2 - S_1$ and $S_n - S_{n-1}$ internal conversion occurs very rapidly (ps) and is the most likely de-excitation process of higher singlet states (xi). $T_2 - T_1$ and $T_n - T_{n-1}$ internal conversion is also spin-allowed rapid process (xii). $S_1 - T_1$ (and $S_1 - T_n$) intersystem crossing are the main population processes of triplet states and are commonly observed (xiv). $T_1 - S_1$ intersystem crossing is possible by thermal activation of T_1 state and is responsible for the phenomenon of *delayed* fluorescence (xvi). $S_n - T_n$ intersystem crossing has been observed for several compounds (xvii). In the following sections, some of the above processes will be described in more detail.

2.6. Absorption lineshape

The result of quantum mechanical considerations for the transition rate between ground and excited electronic states was the Fermi's golden rule:

$$\Gamma_{12} = \frac{\pi}{2\hbar^2} E_0^2 \left|\mu_{12}\right|^2 \delta(\omega_0 - \omega) \qquad (12)$$

Plotting the frequency dependence of the transition rate according to the Eq. (12) would give, contrary to experimental observations, a singular line at ω_0, as shown in the left

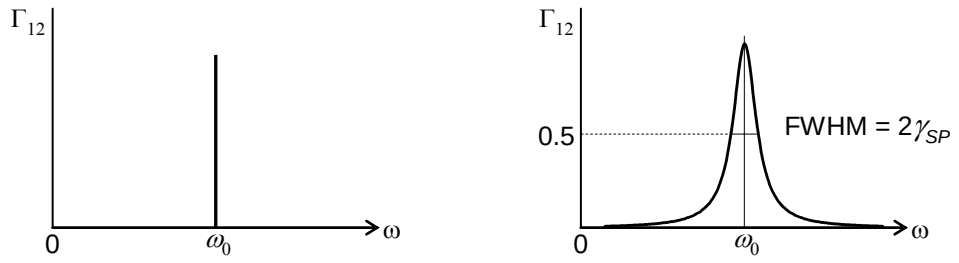

Figure 9

part of Figure 9. This singularity is a consequence of the approximations made during the derivation of the Eq. (12). The correct derivation of the absorption lineshape is more complicated and involves calculation of the overall dipole moment resulting from the interaction of molecular wavefunction with electric field. The dipole moment is, on the other hand, related to refractive index via polarizability. The refractive index would separate into real and imaginary parts, the latter being related to the absorption coefficient.

Instead of following the above procedure we may realize the following property of the Dirac's delta function

$$\delta(\omega_0 - \omega) = \lim_{\gamma \to 0} \frac{\gamma / \pi}{(\omega_0 - \omega)^2 + \gamma^2} \tag{13}$$

The argument of the limit (13) is known as the Lorentzian lineshape function

$$F_L(\omega) = \frac{\gamma_{SP} / \pi}{(\omega_0 - \omega)^2 + \gamma_{SP}^{\ 2}} \tag{14}$$

where γ_{SP} has the meaning of the rate of spontaneous emission. Fermi's golden rule is thus the result of the approximation $\gamma_{SP} \to 0$. The expression for the transition rate which includes the proper frequency dependence should be written as

$$\Gamma_{12} = \frac{\pi}{2\hbar^2} E_0^2 |\mu_{12}|^2 \frac{\gamma_{SP} / \pi}{(\omega_0 - \omega)^2 + \gamma_{SP}^{\ 2}} \tag{15}$$

The Lorentzian lineshape of the transition rate is shown in the right part of the Fig. 9. The full width at half maximum (FWHM) of the line corresponds to twice the rate of the spontaneous emission which, in turn, is related indirectly to the radiative lifetime. Shortening of the radiative lifetime thus causes broadening of the absorption line, an effect known as *radiative broadening*.

2.7. Absorption vibronic transitions

The treatment of absorption in Chapter 1 was simplified by concentrating on electron wavefunctions and states and neglecting the effect of the vibration motion of atomic nuclei. Such treatment is possible in the so-called *Born-Oppenheimer approximation*, which takes into account the fact that electrons, because of their much smaller mass, move much faster than the vibrating nuclei. It is thus possible to completely neglect the coupling between the nuclear motion and electron distribution. The total wavefunction of a state $\Psi(\mathbf{r},\mathbf{R})$ can be written as a product of the electronic wavefunction $\psi(\mathbf{r})$ and nuclear wavefunction $\chi(\mathbf{R})$:

$$\Psi(\mathbf{r},\mathbf{R}) = \psi(\mathbf{r})\chi(\mathbf{R}) \tag{16}$$

As the vibration motion of nuclei does affect the energy levels of electrons, the wavefunction (16) should be now used instead of the simple electron wavefunctions in the expression for the transition dipole matrix element (5), where the operator $\boldsymbol{\mu}$ now has the form

$$\boldsymbol{\mu} = -e\sum_i \mathbf{r}_i + e\sum_j Z_j \mathbf{R}_j \tag{17}$$

The transition dipole matrix element is then

$$\boldsymbol{\mu}_{12} = \int \psi_2^* \chi_2^* \left(-e\sum_i \mathbf{r}_i + e\sum_j Z_j \mathbf{R}_j \right) \psi_1 \chi_1 dr dR \tag{18}$$

which can be separated as

$$\boldsymbol{\mu}_{12} = -e\int \psi_2^* \sum_i \mathbf{r}_i \psi_1 dr \int \chi_2^* \chi_1 dR + e\int \psi_2^* \psi_1 dr \int \chi_2^* \sum_j Z_j \mathbf{R}_j \chi_1 dR \tag{19}$$

Due to orthogonality of the electronic wavefunctions the second element on the right is zero and the matrix element can be written as

$$\boldsymbol{\mu}_{12} = \int \chi_2^* \chi_1 dR \int \psi_2^* \boldsymbol{\mu} \psi_1 dr \tag{20}$$

The transition probability derived in Chapter 1 is thus modulated by a factor depending on the overlap of the nuclear vibrational wavefunctions, which are usually approximated by quantum oscillators. Since the transition rate is proportional to the square of the matrix element (20), it is customary to denote

$$S(\chi_2, \chi_1) = \left| \int \chi_2^* \chi_1 dR^2 \right| \qquad (21)$$

The quantity $S(\chi_2, \chi_1)$ is called *Franck-Condon factor* of an electronic transition.

Similar reasoning leads to the formulation of Franck-Condon principle: *Because the electronic transition takes place much faster than the vibrational motion of nuclei, the most probable transition occurs between states with the same nuclear coordinates (position).*

The principle can be illustrated using the scheme of Figure 10. Instead of simple horizontal lines as in the Jablonski diagram, the electronic state potential energies are drawn as anharmonic oscillators. The vibrational states of the nuclei now appear as additional set of levels v = 0, 1, 2, … in each electronic state. The scheme also shows the square of the oscillator vibrational wavefunctions for a few vibrational levels. The Franck - Condon principle states that the only transitions possible are those that connect the two electronic states by *vertical arrows*. The scheme also indicates that the most probable transitions to and from higher vibrational levels will be those from the oscillator turning points. At room temperature (and at lower temperatures) the transitions almost exclusively occur from the v = 0 vibrational level of the ground state to v = 0 or higher vibrational levels of the excited state. Each transition which is represented by an arrow in the Fig. 10 appears as a Lorentzian line in the absorption spectrum. Further, the Fig. 10 shows only one vibrational mode v

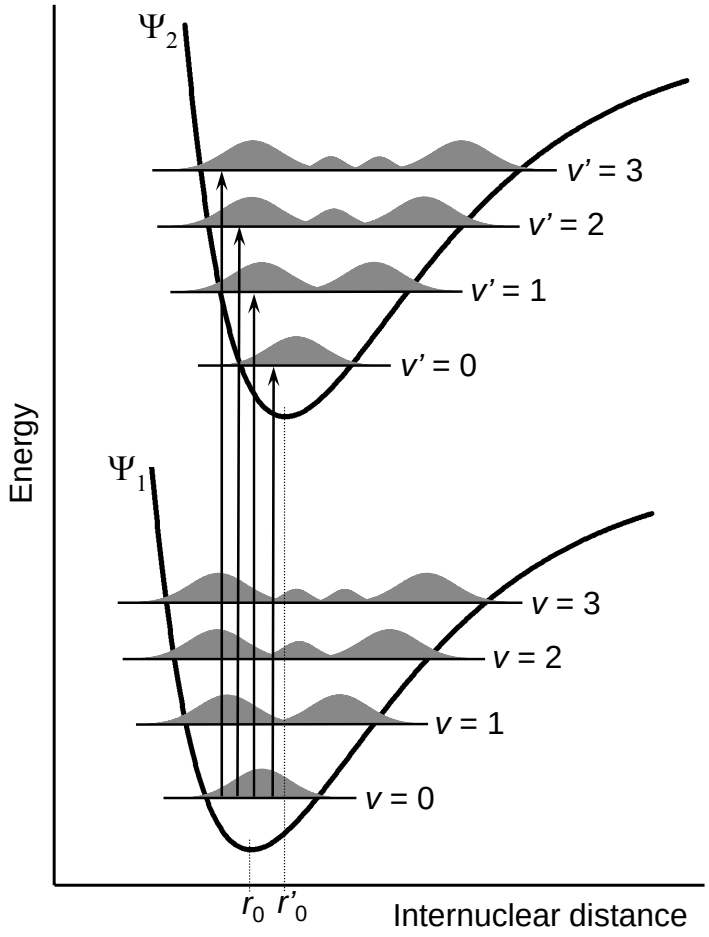

Figure 10

and its overtones. In complex aromatic molecules, there are large numbers of vibrational frequencies v corresponding to the different vibrational modes. Again, each is represented in the absorption spectrum by a narrow Lorentzian line. The overall room-temperature absorption spectrum as commonly observed is an envelope of all vibronic (electronic + vibrational) transitions occurring in the molecule, as shown schematically in Figure 11.

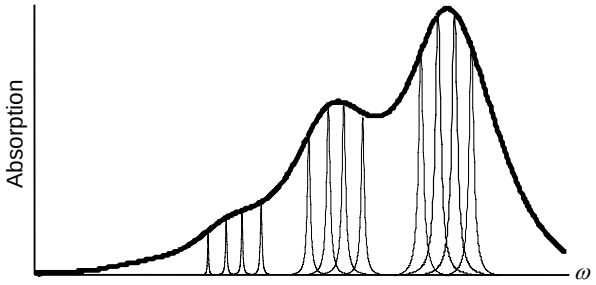

Figure 11

2.8. Absorption: relation to experimental observables

Absorption of light in matter is usually characterized by frequency-dependent *molar absorption (extinction) coefficient* $\varepsilon(\omega)$, expressed usually in units of [L.mol^{-1}.cm^{-1}]. According to Beer's law,

$$\frac{dI}{dl} = -\varepsilon(\omega) IC \qquad (22)$$

where C is sample concentration, l length and I light intensity. Another quantity often used in relation to absorption is absorption cross-section $\sigma(\omega)$, in units [cm^2]. $\sigma(\omega)$ is related to Beer's law as:

$$\frac{dI}{dl} = -\sigma(\omega) In \qquad (23)$$

where n is the number of molecules in unit volume. However, since Eq. (22) is usually solved using decade logarithm and Eq. (23) using natural logarithm, the relationship between the two quantities is

$$\sigma(\omega) = 2.303\varepsilon(\omega) / N_A \qquad (24)$$

with N_A the Avogadro's constant. It is possible to show that the integrated absorption coefficient is related to the transition dipole matrix element as

$$A = \int \varepsilon(\omega) d\omega = \frac{2\pi^2 N_A \omega_0}{3\varepsilon_0 \hbar c \ln(10)} \left|\mu_{12}\right|^2 \qquad (25)$$

where c is speed of light.

The frequency dependence of the absorption coefficient is called an *absorption spectrum*. The practical amount of information that can be obtained from conventional absorption spectrum is usually limited by the complexity of electronic and vibrational states and by various processes that cause broadening of the originally sharp electronic transitions. Mostly, it is possible to assign absorption bands to individual singlet states S_1, S_2. …, and obtain Franck-Condon factors for limited electronic-vibrational (*vibronic*) transitions. An example of absorption spectra of a series of aromatic compounds (acenes) is shown in Figure 12. The spectra nicely illustrate the effect of the size of the conjugated aromatic system (perimeter length l) on the energy of the system. The spectra of the largest compounds, pentacene and tetracene, also show well resolved vibronic structure.

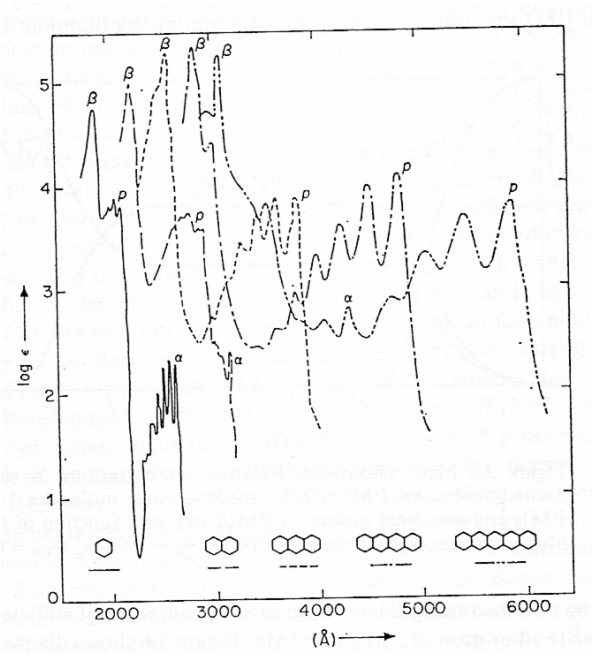

Figure 12 (reprinted from [5])

2.9. Fluorescence spectra

Fluorescence transition $S_1 - S_0$ is an inverse process to the absorption transition $S_0 - S_1$. In absorption, the transitions occur from the 0 vibrational level of the ground state to 0 or higher vibrational levels of the excited state. For aromatic molecules in a condensed medium (liquid solution or solid matrix), the excited state vibrational populations quickly relax to the 0 vibrational level of the excited state due to collision interactions or exchange of phonons. In most cases, absorption into higher excited states S_n is followed by relaxation into the first singlet S_1. Thus, fluorescence process proceeds (apart from a few exceptions) from the 0 vibrational level of the first excited state to 0 or higher vibrational levels of the ground singlet state. This observation is

sometimes called *Kasha's rule*.

Fluorescence *quantum efficiency* ϕ_F is defined as

$$\phi_F = n_F / n_A \tag{26}$$

where n_A is the number of photons absorbed by a molecule per time, and n_F number of photons per time emitted as fluorescence by the molecule. Fluorescence spectrum $F(\omega)$ is then defined as relative fluorescence quantum efficiency at frequency ω:

$$\phi_F = \int_0^\infty F(\omega) d\omega \tag{27}$$

If the vibrational wavefunctions and energies in ground and excited states were same (which, approximately, is the case of polyatomic molecules), the process of absorption and fluorescence would give rise to the phenomenon of mirror symmetry between the absorption and fluorescence spectra, as shown in Figure 13.

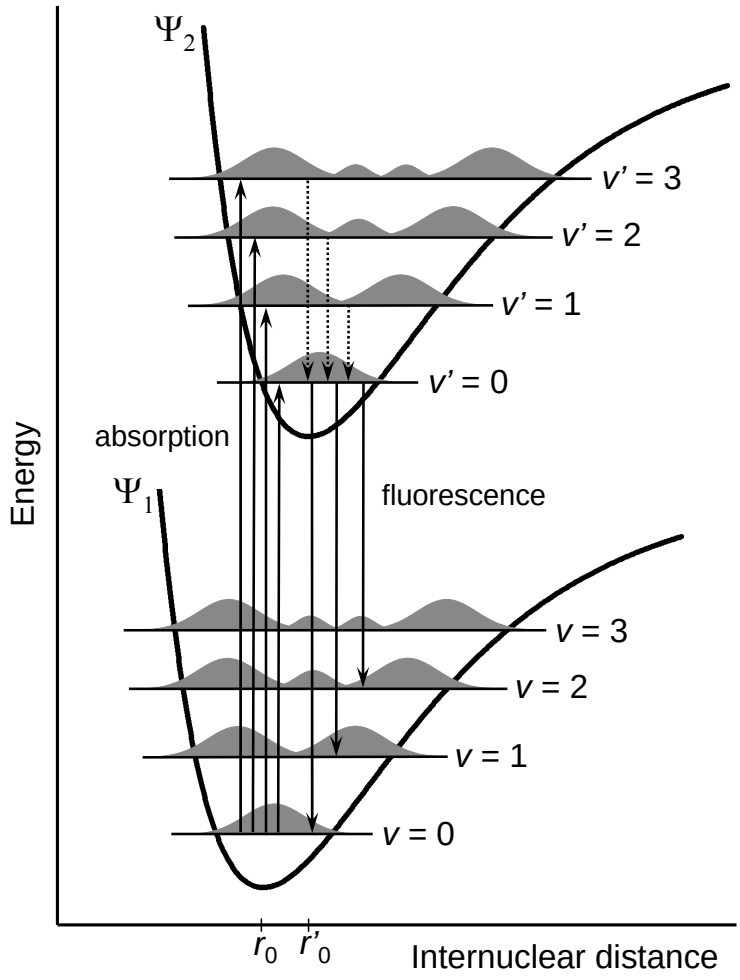

Figure 13

The mirror symmetry rule can be also reasoned theoretically considering the relations

$$\boldsymbol{\mu}_{12} = \int \chi^*_{2v'} \chi_{10} dR \int \psi^*_2 \boldsymbol{\mu} \psi_1 dr \tag{28}$$

for absorption and

$$\boldsymbol{\mu}_{21} = \int \chi^*_{1v} \chi_{20} dR \int \psi^*_1 \boldsymbol{\mu} \psi_2 dr \tag{29}$$

for fluorescence. Compared to Eq. (20), the vibrational wavefunctions are written with the additional quantum numbers 0 and *v*, *v'* to distinguish the vibrational states. Since, as was shown in Chapter 1, the electronic parts of (28) and (29) are symmetric

$$|\mu_{12}|^2 = |\mu_{21}|^2 \quad \text{if} \quad \left| \int \chi^*_{2v'} \chi_{10} dR \right|^2 = \left| \int \chi^*_{1v} \chi_{20} dR \right|^2 \tag{30}$$

which is satisfied if $\chi_{10} = \chi_{20}$ and $\chi_{1v} = \chi_{2v'}$. This is the condition for observation of mirror symmetry between absorption and fluorescence spectra.

This phenomenon of mirror symmetry can be observed experimentally for many systems. An example is shown in Figure 14. The difference between the maxima of the lowest energy absorption and highest energy fluorescence bands, called *Stokes shift*, is an important parameter related to the reorganization energy of the molecule.

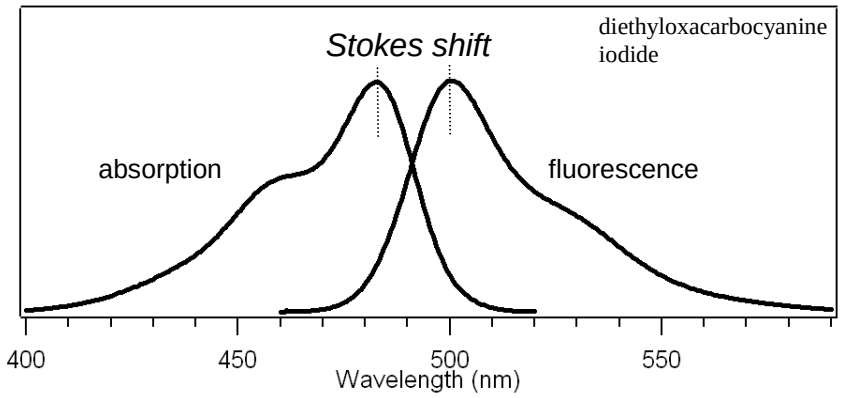

Figure 14

2.10. Fluorescence lifetime

Let us consider a number of molecules M in their excited states; we can express their concentration at time $t = 0$ as $[M^*]_0$. Such excited state can be prepared by irradiating with a strong short laser pulse. The fluorescence intensity I_F will be proportional to the concentration $[M^*]$ at any given time. We can now write a rate

equation

$$\frac{d[M^*]}{dt} = -k_F[M^*] \tag{31}$$

with the solution

$$[M^*] = [M^*]_0 \exp(-t/\tau_F) \quad \text{or} \quad I_F(t) = I_F(0)\exp(-t/\tau_F) \tag{32}$$

where $\tau_F = 1/k_F$ is *fluorescence lifetime*. Fluorescence lifetime is related to the radiative lifetime τ_R defined in Chapter 1 as

$$\frac{1}{\tau_F} = \frac{1}{\tau_R} + \frac{1}{\tau_{NR}} \tag{33}$$

where $\tau_{NR} = 1/k_{NR}$ are lifetime and rate of non-radiative processes competing with fluorescence. It follows that fluorescence quantum efficiency

$$\phi_F = \frac{k_R}{k_R + k_{NR}} = \frac{\tau_F}{\tau_R} \tag{34}$$

The Eqs. (32)-(34) describe generally the effect of non-radiative processes on the relaxation of the excited state. The non-radiative phenomena may include not only intramolecular processes but also itermolecular interactions.

2.11. Radiationless transitions

The most commonly encountered radiationless transitions are singlet-singlet internal conversion $S_n - S_1$ (on timescales of ~10^{-11} s), thermal relaxation of higher vibrational states within the same electronic state (~10^{-12} s), and intersystem crossing $S_1 - T_1$. While the former two processes contribute to the population of the emitting 0 vibrational level of the S_1 state, the latter process is one of the causes of fluorescence quenching.

Apart from intersystem crossing $S_1 - T_1$, fluorescence can be *internally* (intra-molecularly) quenched by $S_1 - T_n$ intersystem crossing and $S_1 - S_0$ internal conversion. The general internal quenching rate k_{NR} introduced in the previous section is thus composed of the intersystem crossing rate k_{ISC} (of both $S_1 - T_1$ and $S_1 - T_n$) and internal conversion rate k_{IC}:

$$k_{NR} = k_{ISC} + k_{IC} \tag{35}$$

It has been found experimentally that k_{NR} is temperature dependent as

$$k_{NR} = k_{NR}^{0} + k'_{NR} \exp(-E_{NR} / kT) \tag{36}$$

where $k_{NR}{}^{0}$ is independent of temperature and the temperature-dependent part is described by an activation energy E_{NR}. In most aromatic molecules the k_{IC} does not depend on temperature because the $S_1 - S_0$ gap is much larger than kT, and the temperature dependence of k_{NR} can be attributed to thermally activated $S_1 - T_n$ intersystem crossing. For benzene and its derivatives, on the other hand, the $S_1 - S_0$ proceeds via an isomeric state and is the main contribution to the temperature dependent part of k_{NR}.

Theoretical treatment of internal conversion has to go beyond the Born-Oppenheimer approximation. The electronic wavefunctions ψ_l, ψ_u (where the subscripts *l*, *u* stand for lower and upper) are thus no longer independent of nuclear coordinates. In organic molecules, the high density of vibrational states merges into a continuum of states, and we may drop the vibrational quantum numbers for the vibrational wavefunctions χ_l, χ_u. The matrix element responsible for the internal conversion becomes

$$H_{lu} = \int \psi_l^*(E_l)\chi_l^*(E) J_N \psi_u(E_u)\chi_u(0) dR \tag{37}$$

where E_l, E_u are electronic state energy levels in zero-vibrational states, E is the vibrational energy of the upper state and J_N is nuclear kinetic energy operator. The matrix element is negligible except for cases when $E_u - E_l \cong E$. The rate constant for the non-radiative transition by internal conversion can be then written as

$$k_{NR} = \left| \int \psi_l^* J_N \psi_u dR \int \chi_l^* \chi_u dR \right|^2 \rho(E) \tag{38}$$

where $\rho(E)$ is density of vibrational states of the lower electronic state. Eq. (38) is formally similar to Fermi's golden rule and Eq. (20). The difference is in the interaction Hamiltonian, which is electric dipole for electronic transition and nuclear kinetic energy for radiationless transition. In contrast to absorption or emission, radiationless transition occurs between iso-energetic vibrational states of different electronic states, and in an energy scheme can be represented by a *horizontal* arrow, as shown in Figure 15.

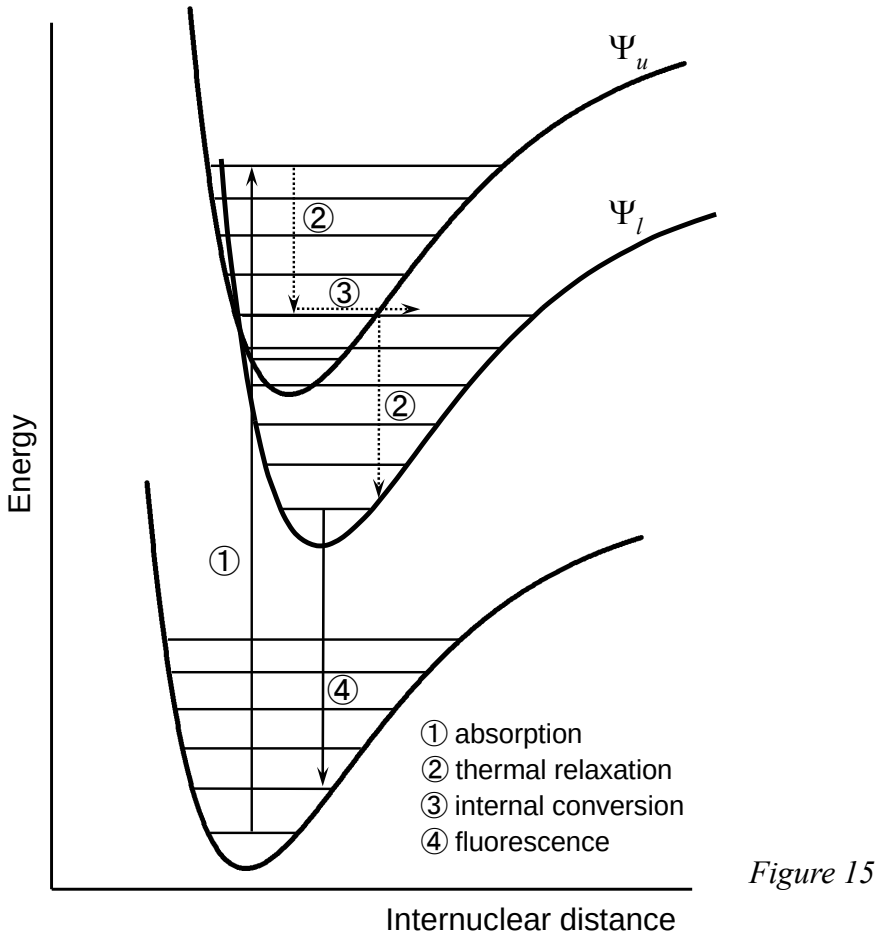

Figure 15

2.12. Phosphorescence

Although phosphorescence refers generally to radiative processes between states of different spin multiplicity, these are in most cases radiative $T_1 - S_0$ transitions. Since the $T_1 - S_0$ transition is electric dipole forbidden, phosphorescence is usually very weak process with long lifetime that can be observed only when other competing nonradiative processes are suppressed. This usually means cooling the sample to cryogenic temperatures to suppress the thermally activated radiationless transitions.

Compared to fluorescence, the quantum characterization of the transition efficiency is more complicated. One possibility is to define *phosphorescence quantum efficiency* ϕ_P as

$$\phi_P = n_P / n_{AT} \tag{39}$$

where n_P is the number of photons emitted as phosphorescence and n_{AT} is the number

of photons absorbed by the molecule that led to the population of the triplet state. Another possibility is to define phosphorescence quantum yield Φ_P as the number of phosphorescence photons n_P divided by the total number of absorbed photons n_A:

$$\Phi_P = n_P / n_A \tag{40}$$

Phosphorescence spectrum $P(\omega)$ is defined as relative phosphorescence quantum efficiency at frequency ω

$$\phi_P = \int_0^\infty P(\omega) d\omega \tag{41}$$

To discuss the transient behavior, let us consider pulsed light excitation that produces concentration of singlet excited states $[^1M^*]_0$ at time $t = 0$. The rate equations of the subsequent processes can be written as

$$\frac{d\left[^1M^*\right]}{dt} = -k_F\left[^1M^*\right] \tag{42}$$

$$\frac{d\left[^3M^*\right]}{dt} = k_{ISC}\left[^1M^*\right] - k_P\left[^3M^*\right] \tag{43}$$

where the superscript 3 in Eq. (43) refers to the triplet state. Applying the initial condition $[^3M^*]_0 = 0$, Eqs. (42) and (43) can be solved to obtain

$$\left[^3M^*\right] = \frac{k_{ISC}\left[^1M^*\right]_0}{\left(k_F - k_P\right)}\left\{\exp(-k_P t) - \exp(-k_F t)\right\} \tag{44}$$

Upon usual conditions, $k_F >> k_P$ and (34) simplifies to

$$\left[^3M^*\right] = \frac{k_{ISC}\left[^1M^*\right]_0}{\left(k_F\right)}\exp(-k_P t) = \left[^3M^*\right]_0 \exp(-k_P t)$$

or $$I_P(t) = I_P(0)\exp(-k_P t) \tag{45}$$

in terms of phosphorescence intensity I_P. The *phosphorescence lifetime* or *triplet lifetime* is given by

$$\tau_P = 1/k_P \tag{46}$$

The actual values of phosphorescent lifetimes vary from miliseconds to tens of seconds. Phosphorescence spectra are shifted to lower energies from fluorescence and $S_0 - S_1$

absorption bands. A few examples of phosphorescence spectra of simple aromatic molecules are shown in Figure 16.

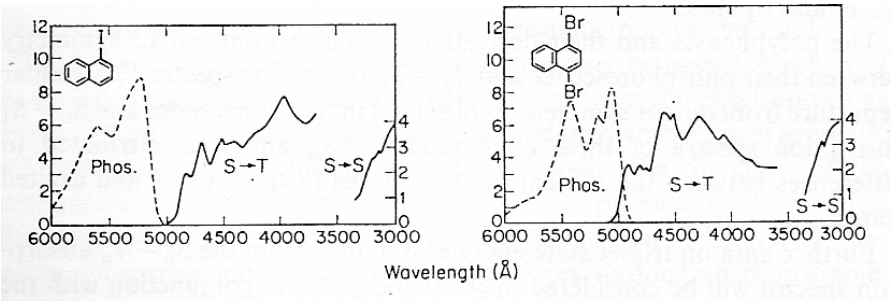

Figure 16 (reprinted from [5])

The fact that it is possible to observe phosphorescence from T_1 level even though the $T_1 - S_0$ transition is spin-forbidden is due to the spin-orbital interactions between the singlet and triplet wavefunctions. The strength of this interaction increases with increasing atomic number *Z*. Aromatic molecules contain only light atoms and their multiplicity forbiddenness factor f_F (defined as ratio of the allowed to forbidden transition intensities) is on the order of 10^8. The spin-orbital interaction can be increased by substitution of atoms with higher *Z*, a phenomenon called *internal heavy atom effect*. Another method of increasing the spin-orbital coupling and the f_F factor is using heavier atom substitutes in the solvent molecules. Such effect is known as *external heavy atom effect*. The external heavy atom effect in $S_0 - T_1$ absorption is shown in Figure 17. Another example of heavy atom induced increase of phosphorescence emission are metal-to-ligand charge transfer states of organometallic complexes containing Ru, Ir, Pt and other metals. In such system, the quantum yield of phosphorescence may reach more than 0.5 and the lifetime is on the order of microseconds.

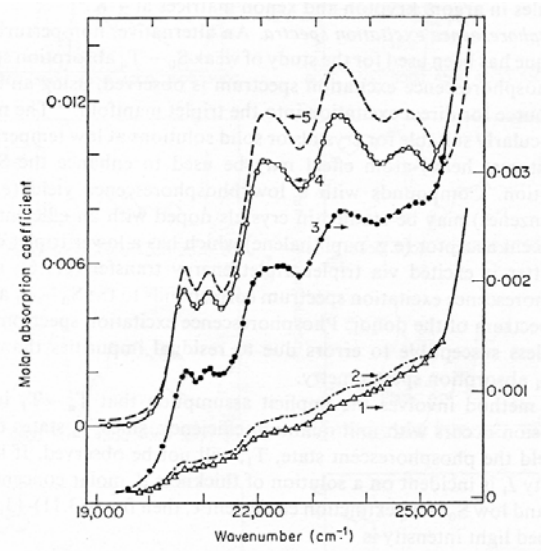

Figure 6.4 External heavy-atom effect. $S_0 - T_1$ absorption spectra of 1-chloronaphthalene (20 cm path) as 1, pure liquid; 2, 1:2 volume fraction in CCl_4; 3, 1:2 volume fraction in $C_2H_4Br_2$; 4, 1:2 volume fraction in C_2H_5I; 5, 1:4 volume fraction in C_2H_5I (after McGlynn, Azumi and Kasha[27])

Figure 17 (reprinted from [5])

3. Molecular complexes

In this chapter, we will be interested in photophysical effects arising from intermolecular interactions. By complexes are meant weakly bound numbers of identical or different molecules N in well-defined geometrical arrangements. The number N can range from 2 for molecular dimers to ~ 1000 for molecular aggregates or conjugated polymers. Molecular complexes can be widely divided into ground-state complexes which are formed in the molecular ground states and keep their arrangement regardless of the presence of light, and excited-state complexes which are formed only after the absorption of light by one of the constituent molecules.

3.1. Ground-state complexes: general considerations

Ground-state complexes are held together by weak intermolecular forces (van der Waals interactions, hydrogen bonds). In such systems, the intermolecular electron orbital overlap and electron exchange are negligible. Electrons responsible for optical transitions are localized on the constituent molecules, and the molecular units of the system retain their individual characteristics. The theoretical treatment of the electronic states of the complexes can thus proceed in terms of the electronic states of individual isolated molecules.

It should be noted that that the theory presented here treats the *photophysical* properties of the complexes, that is changes in electronic wavefunctions and energies that occur upon absorption of light. The theory does not deal explicitly with the origin of the attractive interactions in the ground states, but may add them as parameters. As a result, the theory can be also applied to electronic transitions in conjugated polymers, in which the monomer units are joined together by strong covalence bonds, but in which, from the point-of-view of interactions with light, each conjugated segment can be treated as an isolated molecule only weakly interacting with its neighbors.

3.2. Molecular dimer

Theoretical treatment of the wavefunctions and energies of a molecular dimer can be based on the Born-Oppenheimer approximation. The justification for the use of this approximation will be given later. As a result, the effect of molecular vibrations appears in the form of Franck-Condon factors that modify the matrix elements of electronic transitions. We can, therefore, proceed with the theory of electronic states separated

from the vibrational states.

The treatment of the dimer will be eventually extended to aggregates of larger numbers of molecules. The notation used in this Chapter will be therefore different from the one used in the Chapter 1 and the same symbols will have different meanings in the two Chapters. We will consider only two electronic levels of the constituent monomer molecules. Their ground state wavefunctions will be ψ_1, ψ_2, where the numerical subscripts refer to the different molecules no. 1 and 2. The wavefunctions of their excited states will be written with the superscript *u* (upper) as ψ_1^u, ψ_2^u. The ground state wavefunction of the dimer is a product of the monomer wavefunctions

$$\Psi_G = \psi_1 \psi_2 \qquad (1)$$

Similar consideration leads to two possible non-stationary excited states either with molecule 1 or molecule 2 excited

$$\psi_1^u \psi_2 \quad \text{or} \quad \psi_1 \psi_2^u \qquad (2)$$

Since the two molecules are indistinguishable, the excited state wavefunctions has to be written as linear combinations of (2)

$$\Psi_E = a\,\psi_1^u \psi_2 + b\,\psi_1 \psi_2^u \qquad (3)$$

with the coefficients *a*, *b* to be determined later. The Hamiltonian operator of the dimer is

$$H = H_1 + H_2 + V_{12} \qquad (4)$$

where H_1 and H_2 are Hamiltonians for the isolated monomers and V_{12} is an operator for the intermolecular interaction. Using the Hamiltonian (4) in the time-independent Schrödinger equation for the dimer ground state

$$H\Psi_G = E_G \Psi_G \qquad (5)$$

we obtain for the dimer ground state energy

$$E_G = \iint \psi_1 \psi_2 H \psi_1 \psi_2 dr_1 dr_2 = E_1 + E_2 + \iint \psi_1 \psi_2 V_{12} \psi_1 \psi_2 dr_1 dr_2 = E_1 + E_2 + D_G \qquad (6)$$

where we have, for simplicity, omitted the notation for complex conjugation. The terms E_1 and E_2 are ground state energies of the isolated monomer and D_G is energy correction due to van der Waals interaction in the ground state, lowering the E_G. Writing the Schrödinger equation for the states (3) we obtain

$$H\Psi_E = E_E\Psi_E \quad \text{or} \quad H\left(a\psi_1^u\psi_2 + b\psi_1\psi_2^u\right) = E_E\left(a\psi_1^u\psi_2 + b\psi_1\psi_2^u\right) \tag{7}$$

Multiplying (7) from left alternately by $\psi_1^u\psi_2$ and $\psi_1\psi_2^u$ and integrating each time over coordinates of both molecules leads to a system of two equations

$$\begin{aligned} aH_{11} + bH_{12} &= aE_E \\ aH_{21} + bH_{22} &= bE_E \end{aligned} \tag{8}$$

where we have denoted

$$H_{11} = \iint \psi_1^u\psi_2 H \psi_1^u\psi_2 dr_1 dr_2 \tag{9}$$

$$H_{12} = \iint \psi_1^u\psi_2 H \psi_1\psi_2^u dr_1 dr_2 \tag{10}$$

It follows from the symmetry of the problem that $H_{11} = H_{22}$ and $H_{12} = H_{21}$. Requiring that the determinant of (8) be zero

$$\begin{vmatrix} H_{11} - E_E & H_{12} \\ H_{12} & H_{11} - E_E \end{vmatrix} = 0 \tag{11}$$

gives two excited energy states in the form of

$$E'_E = H_{11} + H_{12} \quad \text{and} \quad E''_E = H_{11} - H_{12} \tag{12}$$

and two corresponding wavefunctions,

$$\Psi'_E = 1/\sqrt{2}\left(\psi_1^u\psi_2 + \psi_1\psi_2^u\right) \quad \text{and} \quad \Psi''_E = 1/\sqrt{2}\left(\psi_1^u\psi_2 - \psi_1\psi_2^u\right) \tag{13}$$

Evaluating Eqs. (12) using the Hamiltonian (4) we obtain

$$\begin{aligned} E'_E &= E_1^u + E_2 + \iint \psi_1^u\psi_2 V_{12}\psi_1^u\psi_2 dr_1 dr_2 + \iint \psi_1^u\psi_2 V_{12}\psi_1\psi_2^u dr_1 dr_2 \\ E''_E &= E_1^u + E_2 + \iint \psi_1^u\psi_2 V_{12}\psi_1^u\psi_2 dr_1 dr_2 - \iint \psi_1^u\psi_2 V_{12}\psi_1\psi_2^u dr_1 dr_2 \end{aligned} \tag{14}$$

The first integral on the right side of the equations (14) represents the van der Waals interaction between an excited state molecule 1 and ground state molecule 2. The last term in both equations is called *exciton displacement* or *exciton splitting* term. It describes the transition of, or exchange of, excitation from molecule 1 to molecule 2.

Using convenient symbols, the equations (14) can be rewritten as

$$E'_E = E_1^u + E_2 + D_E + \varepsilon$$

$$E''_E = E_1^u + E_2 + D_E - \varepsilon \qquad (15)$$

We have seen thus so far, that the interaction between two molecules brings about lowering of their combined ground state energy by van der Waals interaction, and lowering and splitting of their excited state energy due to interaction with light. The result is schematically shown in Figure 18.

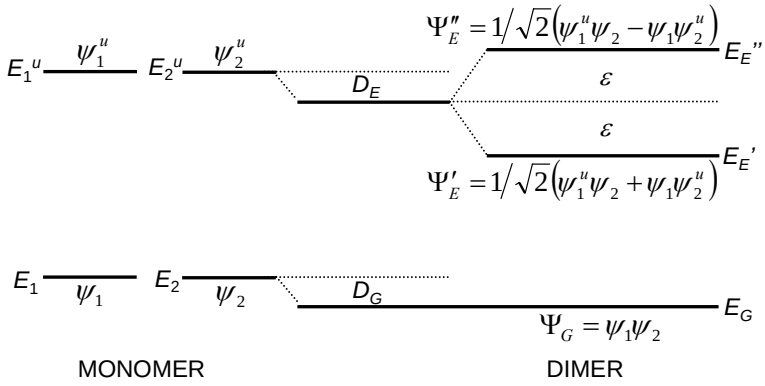

Figure 18

In terms of the optical transition energies between the excited and ground states we can write

$$E_E - E_G = \Delta E = \Delta E_{monomer} + \Delta D \pm \varepsilon \qquad (16)$$

To proceed further, we now have to specify the form of the van der Waals interaction Hamiltonian V_{12}. Generally, this operator includes Coulomb interaction between all electrons and nuclear particles of the interacting molecules. Using such operator, the relevant terms cannot be easily evaluated. Instead, the operator is usually expanded into a series of multipoles, containing monopole-monopole, monopole-dipole, dipole-dipole, quadrupole-quadrupole, and higher interactions. For neutral molecules the interactions involving monopoles are zero, and for allowed optical transitions the dipole-dipole interaction is the dominating term. In a coordinate system where the transition is oriented along axis *x* and *z* is taken as the intermolecular axis, the operator has the form

$$V_{12} = \frac{e^2}{4\pi\varepsilon_0 r_{12}^3}\sum_{i,j} x_1^i x_2^j \qquad (17)$$

where each molecule is treated as an electric dipole, r_{12} is the intermolecular distance and $x_1{}^i$ are the coordinates of electron i of molecule 1. The geometry of the above

operator corresponds to the parallel (also face-to-face or card-pack) type of dimer molecule. The structure is schematically shown in Figure 19.

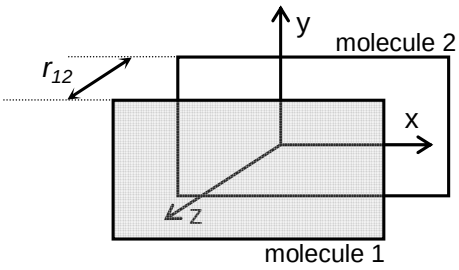

Figure 19

Using the potential (17) we may now attempt to evaluate the exciton displacement term ε.

$$\varepsilon = \iint \psi_1^u \psi_2 V_{12} \psi_1 \psi_2^u dr_1 dr_2 = \frac{1}{4\pi\varepsilon_0 r_{12}^3} \int \psi_1^u \left(\sum_i ex_1^i \right) \psi_1 dr_1 \int \psi_2^u \left(\sum_j ex_2^j \right) \psi_2 dr_2 \quad (18)$$

In the integrals in Eq. (18) we may recognize the *transition dipole moments* of individual monomer molecules (as introduced in Chapter 1, Eq. (25)). Using μ_1, μ_2 for the transition dipole moments of molecules 1 and 2, we may write

$$\varepsilon = \frac{\mu_1 \mu_2}{4\pi\varepsilon_0 r_{12}^3} \quad (19)$$

for the case of an interaction of identical molecules. While both transition moments are oriented along the *x*-axis, their direction may be chosen arbitrarily. To confirm with the Fig. 14 (i.e. to ensure that Ψ'_E is the wavefunction with lower energy) we set

$$\boldsymbol{\mu}_1 = -\boldsymbol{\mu}_2 \quad (20)$$

The reason for this choice will be obvious later.

3.3. Selection rules for optical transitions in molecular dimers

Although theoretically there are two distinct excited states in a dimer molecule (predicted from Eq. (15)), both of them may not necessarily take part in an optical transition. It is possible to derive a set of simple geometry-based selection rules which will enable one to determine which dipole transition is allowed by examining the structure of the dipole molecule.

For the example of the parallel dimer discussed above, we may try to evaluate matrix elements of the total electric dipole operator of the dimer molecule. The transition dipoles corresponding to the two excited states are

$$\mathbf{M}' = \iint \Psi_G (\hat{\mu}_1 + \hat{\mu}_2) \Psi'_E dr_1 dr_2$$

and $$\mathbf{M}'' = \iint \Psi_G (\hat{\mu}_1 + \hat{\mu}_2) \Psi''_E dr_1 dr_2 \qquad (21)$$

where $\hat{\mu}_1, \hat{\mu}_2$ are dipole moment *operators* of the monomers. Using the expressions (1) and (13) in Eq. (21) we obtain

$$\mathbf{M}' = 1/\sqrt{2} \int \psi_1 \hat{\mu}_1 \psi_1^u dr_1 + 1/\sqrt{2} \int \psi_2 \hat{\mu}_2 \psi_2^u dr_2 = 1/\sqrt{2} (\boldsymbol{\mu}_1 + \boldsymbol{\mu}_2) \qquad (22)$$

and, similarly,

$$\mathbf{M}'' = 1/\sqrt{2} (\boldsymbol{\mu}_1 - \boldsymbol{\mu}_2) \qquad (23)$$

thus obtaining a simple relationship between the transition dipole moment of the dimer and those of the constituent monomers. For the optical transition to a particular excited state of the dimer to occur, the corresponding transition dipole moment must be non-zero. We have seen that for the parallel dipole $\boldsymbol{\mu}_1 = -\boldsymbol{\mu}_2$, which gives

$$\mathbf{M}' = 0 \qquad \text{and} \qquad \mathbf{M}'' = \frac{2\boldsymbol{\mu}_1}{\sqrt{2}} \qquad (24)$$

Referring to Fig. 14, the absorption to the upper state Ψ''_E is dipole allowed while that to the lower state Ψ'_E is dipole forbidden.

The above simple vector treatment can be extended also to the prediction of the relative energies of different dimer geometries based on the consideration of the energy of two interacting classical electric dipoles. For a parallel dimer, the energy of two dipoles pointing in opposite directions is, due to Coulomb interaction, lower than that of dipoles pointing in the same direction. In contrast, in the serial (or head-to-tail) dimer, the situation is reversed. The arrangement with both dipoles pointing in the same direction has lower energy and the transition is dipole allowed. Thus, based on the knowledge of the geometry of the system, one is able to use vector addition and classical electrostatics to predict the phases of excited state wavefunctions and probability of the transition, as illustrated in Figure 20.

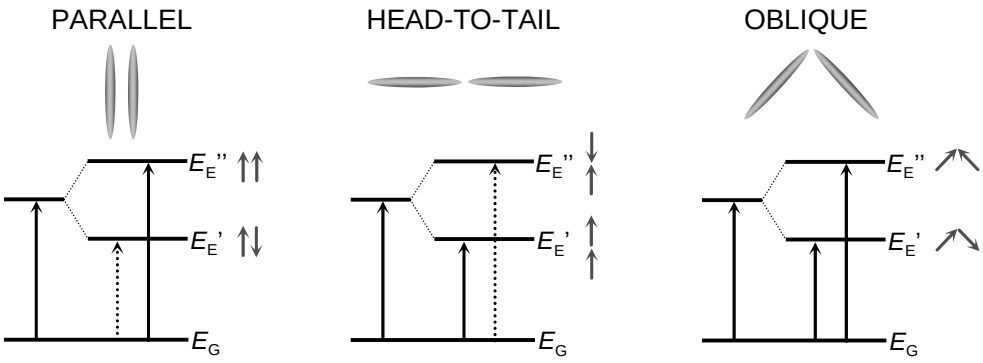

Figure 20

3.4. Molecular aggregates

The theoretical approach developed above for the molecular dimer can be easily extended to the concept of infinite 1-dimensional linear chain, or molecular aggregate. Because of the chain infinite length, the lack of boundary conditions makes the model applicable for very long chains. For aggregates of intermediate length (3 – 10 molecules) the results are not well applicable.

We will assume a linear chain composed of N identical molecules (where N is very large). The ground state wavefunction is a product of the ground state wavefunctions of individual molecules

$$\Psi_G = \psi_1\psi_2\psi_3.....\psi_N = \prod_{n=1}^{N}\psi_n \tag{25}$$

The excited state can be written as

$$\Phi_a = \psi_1\psi_2\psi_3.....\psi_a^u.....\psi_N = \psi_a^u\prod_{\substack{n=1\\ n\neq a}}^{N}\psi_n \tag{26}$$

This is an excited state of the aggregate where the monomer molecule a is excited and other molecules are in their ground states. There are N such products and they represent non-stationary excited states. Generally, we may write the total excited state as a linear combination of the states expressed by (26)

$$\Psi_E^k = \sum_{a=1}^{N} C_{ak}\Phi_a \tag{27}$$

where the coefficient k describes the k^{th} exciton state (notation used instead of the ‘, “ notation for the dimer). Assuming an infinite chain, the magnitude of the coefficients C_{ak} will be same for all a (no boundary effects) and the coefficients will differ only in their phases. This fact can be expressed as

$$\Psi_E^k = \frac{1}{\sqrt{N}} \sum_{a=1}^{N} \exp(2\pi i k a / N) \Phi_a \tag{28}$$

where $k = 0, \pm 1, \pm 2, \ldots .. N/2$.

3.5. The concept of molecular exciton

The Eq. (28) describing the molecular aggregate excited state is a linear combination of excited states of individual monomer molecules represented with equal weights. The effect of the linear combination is that the wavefunction is a wavefunction of a *collective excitation* of N molecules in the chain. The excitation is delocalized over N monomer molecules and possesses well-defined phases for each monomer. This type of excitation is called *molecular exciton*. To distinguish it from the concept of Wanier excitons used in solid state physics, this exciton is also called *Frenkel exciton*. The principle difference from Wanier exciton is that in Frenkel exciton the electrons of the excited states are *localized* on individual monomer molecules. The delocalization mentioned above refers to the *excitation* that is spread over N molecules. The delocalization length (or, equivalently the number N) is called *coherent length* of the exciton.

Following the procedure used to determine the excited state energies of the dimer, it is possible to use the wavefunctions (25) and (27) to calculate the excited energies of the aggregate. The van der Waals interaction potential is again approximated by dipole-dipole interaction, and as further simplification, the interaction is considered to take place only between nearest neighbors. The exciton displacement term of the interaction potential is then expressed as

$$\varepsilon_{a,a+1} = \int \Phi_a V_{a,a+1} \Phi_{a+1} dr \tag{29}$$

which describes the transfer (displacement) of the excitation from state with molecule a excited to state with molecule a+1 excited, that is transfer of excited energy between neighboring molecules. The exciton state energies are given by

$$E_E^k = E_{E,a} + 2\left(\frac{N-1}{N}\right)\cos\left(\frac{2\pi k}{N}\right)\varepsilon_{a,a+1} \qquad (30)$$

where $E_{E,a}$ is the excited state energy of the molecule a, and $k = 0, \pm 1, \pm 2, \ldots\ldots N/2$. The actual form of the dipole-dipole interaction term depends on the geometry of the problem. For a linear chain with translation-equivalent components inclined at an angle α from the chain axis (Figure 21),

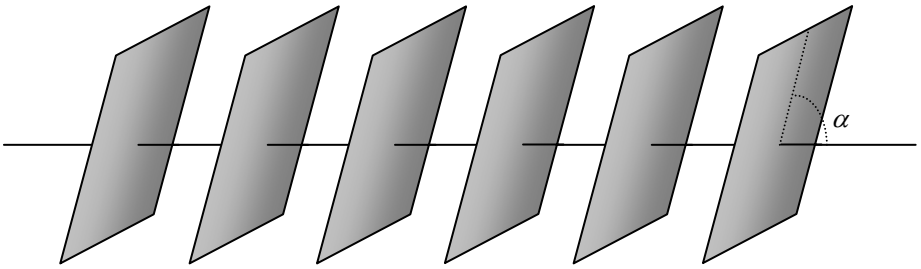

Figure 21

the expression (30) can be written in terms of the monomer transition dipole moment μ as

$$E_E^k = E_{E,a} - 2\left(\frac{N-1}{N}\right)\cos\left(\frac{2\pi k}{N}\right)\left(\frac{\mu^2}{4\pi\varepsilon_0 r^3}\right)\left(1-3\cos^2\alpha\right) \qquad (31)$$

The equations (30), (31) represent *exciton dispersion relations*, that is, dependence of the exciton energy on k. The exciton energy levels calculated from Eq. (31) for a few values of α are shown in Figure 22

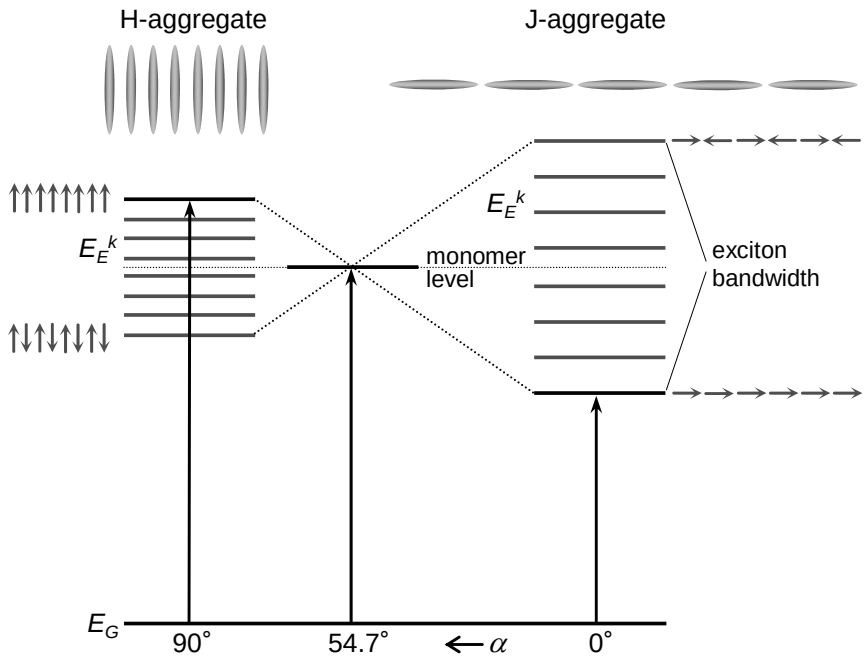

Figure 22

The case for α = 90 corresponds to the card-pack arrangement of molecules, often called *H-type aggregate*. The case of α = 0 is the head-to tail configuration, also called *J-type aggregate*. The Fig. 22 also shows that the same selection rules that were derived for the dimer can be used for the aggregates. Thus, for H-aggregates the transition to the lowest exciton level is forbidden and for J-aggregates this transition is allowed. All intermediate transitions for these two extreme cases are forbidden.

The spread of the exciton energy levels in Fig. 22 is called *exciton band* structure. For an *N*-component aggregate there are *N* energy levels. The *exciton bandwidth* is twice the energy shift component in Eqs. (30) or (31); generally, this has a form

$$bandwidth = 4\left(\frac{N-1}{N}\right)\cos\left(\frac{2\pi k}{N}\right)\varepsilon_{a,a+1} \qquad (32)$$

The exciton bandwidth of a linear infinite chain is twice the bandwidth for the dimer of corresponding structure. This is a result of the nearest-neighbor approximation. Each molecule in a linear chain has two neighbors, and compared to dimer undergoes 2 dipole-dipole interactions. More exact considerations would show that the longer-range interactions cannot be neglected. Inclusion of 8 neighbors on each side brings the factor of aggregate vs. dimer exciton bandwidth to 2.39.

3.6. Spectral properties of molecular aggregates

Spectral properties of molecular dimers and aggregates are determined by their exciton band structure and corresponding selection rules. In absorption, the spectra of H-type dimers and aggregates are shifted to higher energies (blue shift), those of J-type dimers and aggregates to lower energies (red shift). The Kasha's rule stipulates that population of the highest (allowed) exciton level of H-type dimers (aggregates) will quickly non-radiatively relax to the lowest exciton level from where the dipole transition to the ground state is forbidden. The population is thus efficiently transferred to a lower-lying triplet state from where efficient phosphorescence has been observed.

Many cyanine molecules are known to form very large aggregates. Although the total number of molecules in the aggregate does not correspond to the exciton coherent length *N* (due to the presence of deformations and defects along the chain), the values of *N* are still very large (estimates vary between 50 and ~ 1000). Structurally, these are predominantly J-aggregates. The large coherence length gives rise to some characteristic spectral features: sharp red-shifted absorption and luminescence band without vibrational structure, and very short fluorescence lifetime. An example of

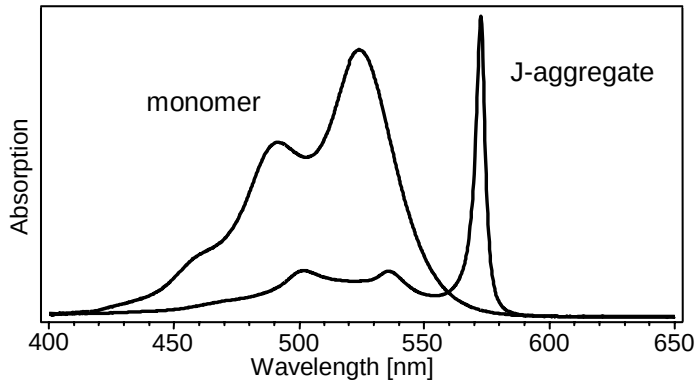

Figure 23

J-aggregate absorption spectra is shown in Figure 23. Lack of the vibrational structure is due to the large delocalization of the excitation. As a result, the relative change of nuclear configuration upon excitation is much smaller than in the case of monomer, and the observed exciton band is a purely electronic 0-0 transition. Further narrowing of the band is a phenomenon called *motional narrowing*. It is caused by the disorder in transition frequencies of individual monomers being averaged by the delocalized exciton. The absorption band is narrowed by a factor of $1/\sqrt{N}$, where N is the exciton coherence length. Shortening of the excited state lifetime is called *superradiance*. Excited state radiative lifetime τ_R of the monomer is shortened by a factor of $1/N$ in an aggregate of the coherent length N.

3.7. Excited state dimer: excimer

Apart from ground state dimers and aggregates, there are examples of molecules that experience the attractive van der Waals interactions only in their excited states. Such systems are called excited state complexes, and in case of dimers, excited state dimers, or *excimers*. Schematic potential energy diagram of two parallel molecules as a function of their intermolecular separation r is shown in Figure 24. Here, R represents the repulsive potential in the ground and excited states, V is the attractive potential in the excited state, D is the resulting excimer potential energy.

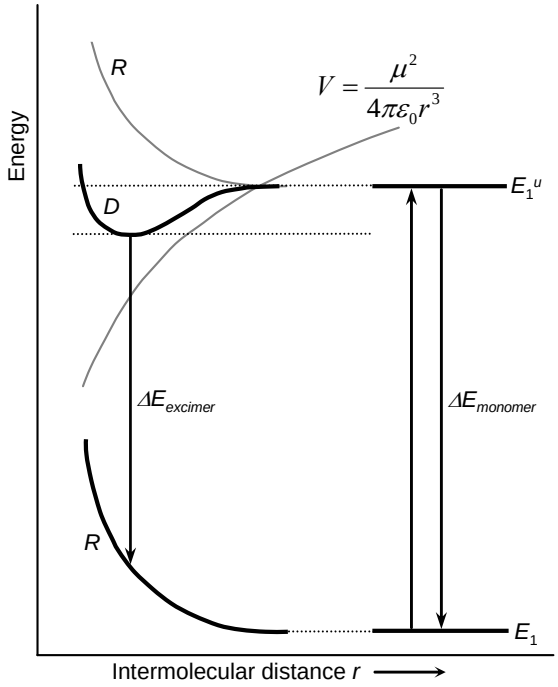

Figure 24

If the excimer energy

$$D = R + V \qquad (33)$$

is lower than the monomer excited state energy at some value of *r*, a bound excimer state can be formed.

In the treatment of ground-state dimers we have explicitly assumed that the repulsive potentials in the ground and excited states were same and dealt only with the attractive interactions. Making the same assumption here, we can basically follow the procedure outlined in Section 3.2. for the dipole-dipole interaction V_{12}. The main difference will be the absence of the term ΔD in the Eq. (16) for the dimer transition energy. We can thus write

$$E_E - E_G = \Delta E_{monomer} + \varepsilon = \Delta E_{monomer} + \frac{\mu^2}{4\pi\varepsilon_0 r^3} \qquad (34)$$

where μ is again the transition dipole moment of the monomer. Spectroscopically, excimers are characterized by *absorption spectra* that are identical to absorption spectra of monomers, and by *fluorescence spectra* that are shifted by the amount $\mu^2 / 4\pi\varepsilon_0 r^3$.

An example of fluorescence spectra of typical excimer system, the molecule of pyrene in solution at increasing concentrations (from G to A), is shown in Figure 25.

The solution of pyrene represents an example of *inter-molecular* excimer. When the two monomers are attached to each other by a chemical bond (alkane chain) the resulting molecule can form an *intra-molecular* excimer state, which is usually accompanied by a large change in the molecular geometry.

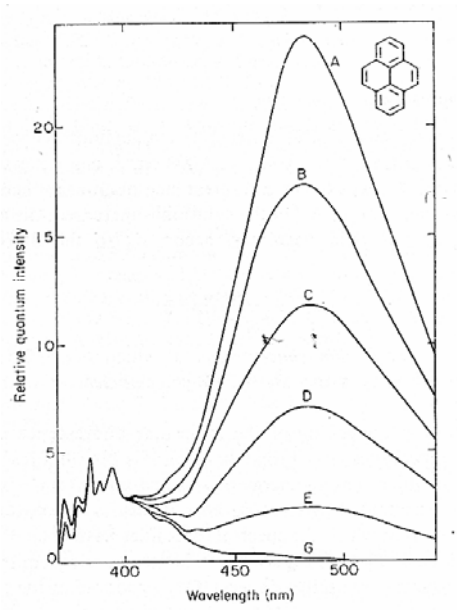

Figure 25 (reprinted from [5])

Fluorescence spectra of pyrene in cyclohexane at concentration between 10^{-2} M (A) and 10^{-4} M (G).

3.8. Charge transfer complexes

In a mixed solution of electron acceptor molecules (from now on denoted as *A*) and electron donor molecules (*D*) one can observe the appearance of a new absorption band due to a *charge-transfer* (CT) state. The pairs of donor and acceptor molecules are accordingly called charge transfer complexes or, alternatively, *donor-acceptor* (DA) *complexes*.

We may characterize the photophysical properties of the CT complexes without going into the details of the mechanism of the charge transfer itself. Let us denote *DA* a neutral donor-acceptor pair, and D^+A^- a pair in which an electron has been transferred from D to A. We can write ground state wavefunction of the complex as a linear combination of the neutral *DA* and charged state D^+A^- wavefunctions as

$$\Psi_G(D,A) = a\Psi_0(DA) + b\Psi_1(D^+A^-) \tag{35}$$

For the excited state wavefunction we can write

$$\Psi_E(D,A) = a^*\Psi_1(D^+A^-) + b^*\Psi_0(DA) \tag{36}$$

The relative magnitudes of the coefficients *a*, *b*, *a**, *b** characterize the strength of the CT complexes. For a weak complex $a \cong a^* \cong 1$ and $b \cong b^* \cong 0$. The optical transition then goes mainly from the neutral state *DA* to the charge transfer state D^+A^- and is called charge transfer transition. For quantitative determination of the character of ground state the ratio

$$\lambda = \frac{b^2}{a^2 + b^2} \tag{37}$$

is often used. Complete charge transfer ground state is characterized by λ = 1, neutral ground state by λ = 0. Without elaborating on the theory of the CT complexes we can write the result for the energy of optical transition as

$$E_{CT} = E_1 - E_0 + \frac{\left(E_{01} - E_1 S\right)^2 + \left(E_{01} - E_0 S\right)^2}{E_1 - E_0} \tag{38}$$

where the matrix element symbols E_0, E_1, E_{01} and S are defined using a complete Hamiltonian H as

$$E_0 = \int \Psi_0 H \Psi_0 dr\,, \quad E_1 = \int \Psi_1 H \Psi_1 dr\,, \quad E_{01} = \int \Psi_1 H \Psi_0 dr \quad \text{and} \quad S = \int \Psi_1 \Psi_0 dr \qquad (39)$$

Alternatively, in terms of macroscopic observables, the transition energy can be expressed as

$$E_{CT} = I_D - A_A - \Delta \qquad (40)$$

where I_D is the ionization potential of D, A_A is the electron affinity of A, and Δ is the difference in the formation energies of the DA complex in excited and ground states (Coulomb interaction between the negative and positive ions). An example of absorption spectrum of a CT complex of dimethylnaphthalene with *p*-chloranil is shown in Fig. 26.

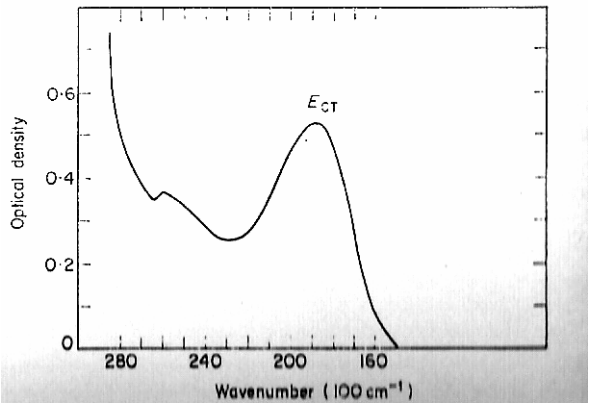

Figure 26 (reprinted from [5])

Similar to excimers, CT complexes can be further divided into inter-molecular complexes (such as the one in Figure 26) and intra-molecular complexes, where the charge transfer occurs between different D and A parts of the same molecule.

3.9. Exciplex

The term exciplex is often used to describe an excited state aggregate of two *different* molecules. As in the case of excimers, the molecules do not interact in their ground states. The principle difference is that while the excimer is bound in its excited state by exciton (dipole-dipole) interaction, the main contribution to the interaction energy of an exciplex comes from a charge transfer character of the excited state.

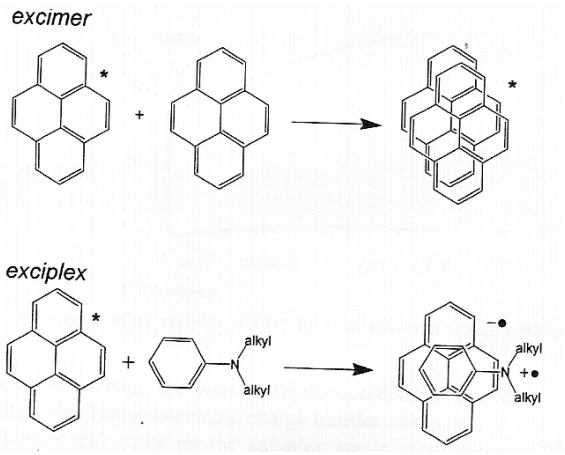

Figure 27 (reprinted from [12])

The situation is schematically shown in Figure 27. It should be noted that the explanation of the excimer interaction in section 3.7. was simplified in the sense that the excited state interaction also includes a small charge transfer contribution. Generally, the excited state wavefunction for excimers and exciplexes should be thus written as

$$\Psi_E = a\Psi_1(D^+A^-) + b\Psi_2(D^-A^+) + c\Psi_3(D^*A) + d\Psi_4(DA^*) \qquad (41)$$

where for excimers $A = D$, $a = -b$ and $c = -d$, with $|a|^2 << |c|^2$.

An example of exciplex emission from the complex of perylene with dimethylaniline is shown in Figure 28. The figure shows, for comparison, also the fluorescence spectrum of the monomer perylene (dotted). As in the case of excimers and CT complexes, exciplexes can be formed either as inter-molecular or intra-molecular complexes.

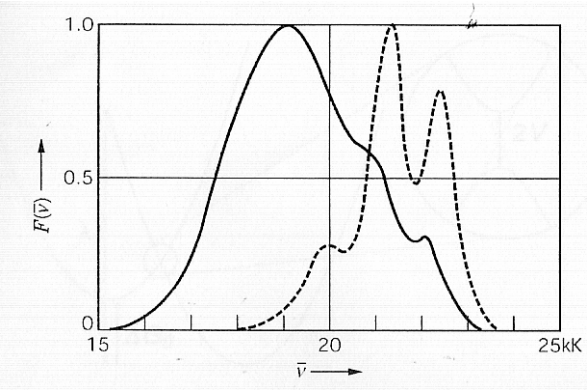

Figure 28 (reprinted from [12])

4. Intermolecular photophysical processes

In the previous Chapter we were interested in weakly-bound systems that interacted *strongly* via dipole-dipole interaction. The result was a coherent excitation delocalized over the system and large shift of the system energy levels. In this Chapter we will treat photophysical processes on pairs of molecules that interact *weakly*, so that each molecule of the pair can be considered as an isolated entity. We will be interested in processes of energy transfer, in which light energy absorbed on one molecule, a donor, is transferred to another molecule, an acceptor.

4.1. Radiative (trivial) energy transfer

The simplest case of energy transfer is the one in which the donor emits a photon, the energy transfers space as light, and is absorbed by an acceptor (Figure 29). Light intensity decreases with distance from the source as r^{-2} (inverse square law) and the radiative energy transfer efficiency follows the same donor-acceptor distance dependence. The probability that a photon emitted by the donor will be absorbed by the acceptor can be expressed as

$$p_{DA} \propto \frac{2.303[A]}{\phi_{FD}} \int F_D(\omega)\varepsilon_A(\omega)d\omega \qquad (1)$$

where $[A]$ is the acceptor concentration, ϕ_{FD} the donor fluorescence quantum efficiency, $F_D(\omega)$ the donor fluorescence and $\varepsilon_A(\omega)$ the acceptor absorption spectra.

At small distances (< ~10 nm) the radiative contribution to energy transfer is negligible compared to the resonant mechanism discussed in the following paragraph. However, radiative transfer can be a dominant mechanism of energy transfer in dilute solutions, where it can influence fluorescence spectra and lifetimes.

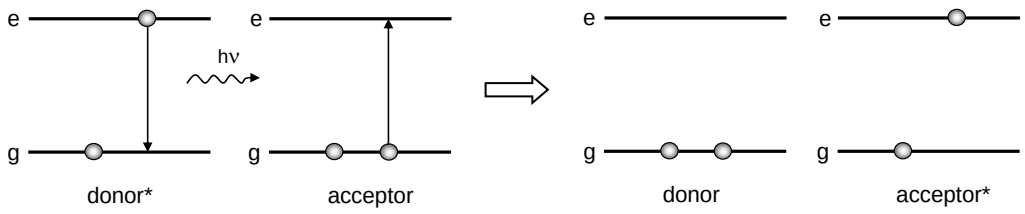

Figure 29

4.2. Förster resonant energy transfer (FRET)

Resonant energy transfer occurs between two molecules via dipole-dipole interaction. The only condition for this process to occur is that the donor and acceptor posses strong transition dipole moments. Due to the spin selection rule this condition usually implies energy transfer between donor singlet and acceptor singlet states. However, as we have seen in Chapter 2, there are cases where the heavy-atom effect can partially lift the spin selection rule and triplet-singlet transitions (such as phosphorescence) can posses significant transition dipole moment. Again, since the strength of the dipole moment is the only relevant parameter governing the resonant energy transfer mechanism, transfer of energy, e.g., between donor triplet and acceptor singlet states can be an efficient process. The resonant energy transfer is schematically depicted in Figure 30.

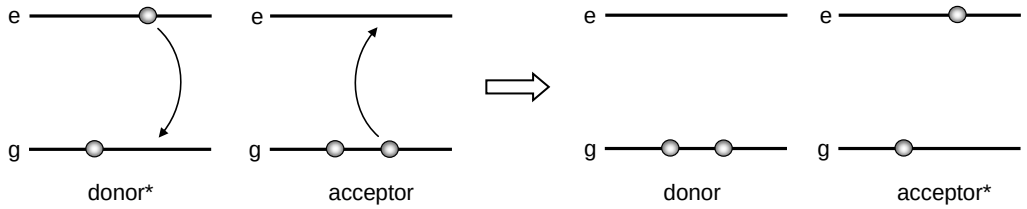

Figure 30

Resonant energy transfer via dipole-dipole interaction is also being called Förster energy transfer after T. Förster who first derived the equation for the energy transfer rate. In deriving the equation, we can begin with a general form of the Fermi's golden rule for the transition rate between two quantum states.

$$\Gamma_{DA} = \frac{\pi}{2\hbar^2}\left|H_{DA}\right|^2 \delta\left(\omega_D - \omega_A\right) \qquad (2)$$

Here, the subscripts D and A refer to the donor and acceptor molecules, respectively, ω_D and ω_A are the transition frequencies, Γ_{DA} is the energy transfer rate constant, and $|H_{AD}|$ is the matrix element of the interaction Hamiltonian. Defining the wavefunctions of the initial i and final f states of the pair of molecules as

$$\Psi_i = \psi_D^u \psi_A \qquad \Psi_f = \psi_D \psi_A^u \qquad (3)$$

where $\psi_D^u \psi_A$ is a state with donor excited and acceptor in ground state and $\psi_D \psi_A^u$ is a

state with donor in the ground state and acceptor excited. Since the dipole-dipole energy transfer takes place uni-directionally over relatively long distances we do not have to take linear combinations of $\psi_D^u\psi_A$ and $\psi_D\psi_A^u$ into account. The matrix element of the interaction Hamiltonian can be then written as

$$|H_{DA}| = \int \Psi_f V_{DA} \Psi_i dr = \int \psi_D \psi_A^u V_{DA} \psi_D^u \psi_A dr \tag{4}$$

The interaction energy operator V_{DA} is due to dipole-dipole interaction between transition dipoles $\boldsymbol{\mu}_D$ and $\boldsymbol{\mu}_A$, or in other words, due to the potential energy of dipole $\boldsymbol{\mu}_A$ in the electric field of the dipole $\boldsymbol{\mu}_D$. From classical electromagnetic theory, the electric field of $\boldsymbol{\mu}_D$ can be written as

$$\mathbf{E}_D = \frac{\boldsymbol{\mu}_D}{4\pi\varepsilon_0 r^3} \tag{5}$$

where ε_0 is permittivity of vacuum. The interaction energy V_{DA} is thus

$$V_{DA} = \mathbf{E}_D \cdot \boldsymbol{\mu}_A = \frac{\boldsymbol{\mu}_D \cdot \boldsymbol{\mu}_A}{4\pi\varepsilon_0 r^3} \tag{6}$$

or for simplicity

$$V_{DA} \propto \frac{\kappa \mu_D \mu_A}{r^3} \tag{7}$$

where r is now distance between the D and A molecules and κ is an orientational factor. With the angles θ_D, θ_A and θ_T defined by Figure 31, the orientational factor can be expressed as

$$\kappa = \cos\theta_T - 3\cos\theta_D \cos\theta_A \tag{8}$$

Depending on the orientation of the dipoles the factor κ can assume values between 4 for parallel orientation and 0 for perpendicular orientation, as shown also in Fig. 28.

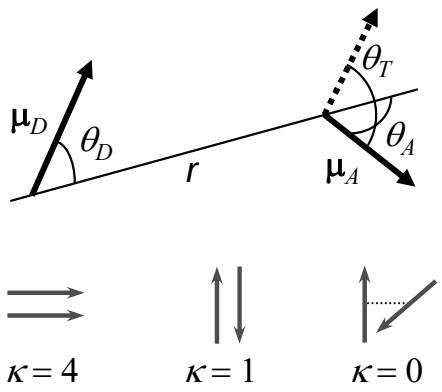

Figure 31

Using now the Eq. (7) in (4) we can write the interaction Hamiltonian as

$$\left|H_{DA}\right| \propto \frac{\kappa}{r^3}\int \psi_D \psi_A^u (\mu_D \mu_A) \psi_D^u \psi_A dr \tag{9}$$

and the energy transfer rate as

$$\Gamma_{DA} \propto \frac{\kappa^2}{r^6}\left|\int \psi_D \psi_A^u (\mu_D \mu_A) \psi_D^u \psi_A dr\right|^2 \delta(\omega_D - \omega_A) \tag{10}$$

Due to the relatively large distance between *D* and *A* the coordinates can be considered independent and the integrand in Eq. (10) can be separated as

$$\Gamma_{DA} \propto \frac{\kappa^2}{r^6}\left|\int \psi_D \mu_D \psi_D^u dr_D\right|^2 \left|\int \psi_A^u \mu_A \psi_A dr_A\right|^2 \delta(\omega_D - \omega_A) \tag{11}$$

Denoting the matrix element of the transition dipole moments of the donor and acceptor molecules as

$$\left|\mu_D\right| = \left|\int \psi_D \mu_D \psi_D^u dr_D\right| \quad \text{and} \quad \left|\mu_A\right| = \left|\int \psi_A^u \mu_A \psi_A dr_A\right| \tag{12}$$

and using the following property of the delta-function

$$\delta(\omega_D - \omega_A) = \int_0^\infty \delta(\omega_D - \omega)\delta(\omega - \omega_A) d\omega \tag{13}$$

we can re-write the Eq. (11) for the transfer rate as

$$\Gamma_{DA} \propto \frac{\kappa^2}{r^6}\int_0^\infty \left|\mu_D\right|^2 \delta(\omega_D - \omega)\left|\mu_A\right|^2 \delta(\omega - \omega_A) d\omega \tag{14}$$

The equation (14) already shows the well-known dependence of the transfer rate on the 6^{th} power of distance *r*. We can further manipulate the equation using the relations

$$\left|\mu_A\right|^2 \delta(\omega-\omega_A) \propto \frac{\varepsilon_A(\omega)}{\omega} \tag{15}$$

which is a consequence of the Eq. (25) of Chapter 2, and

$$\left|\mu_D{}^2\right| \propto B_{12} \propto \frac{A_{12}}{\omega^3} \tag{16}$$

where B_{12} and A_{12} are the Einstein's coefficients, as defined in Eqs. (38) and (43) of Chapter 1. Further,

$$A_{12} = \frac{1}{\tau_R} = \frac{\phi_F}{\tau_F} \tag{17}$$

as seen from Eq. (42) of Chapter 1 and Eq. (34) of Chapter 2. Combining the fluorescence quantum efficiency ϕ_F with the lineshape, as approximated by the delta function $\delta(\omega_D-\omega)$, leads to the fluorescence spectrum

$$\phi_F \delta(\omega_D - \omega) = F_D(\omega) \tag{18}$$

Using the expressions (15-18) in the Eq. (14) we obtain for the energy transfer rate

$$\Gamma_{DA} \propto \frac{\kappa^2}{r^6 \tau_F} \int_0^\infty \varepsilon_A(\omega) F_D(\omega) \omega^{-4} d\omega \tag{19}$$

It is further customary to use a normalized fluorescence spectrum

$$\overline{F}_D(\omega) = F_D(\omega) / \phi_F \tag{20}$$

whereby the equation (19) changes to

$$\Gamma_{DA} \propto \frac{\kappa^2 \phi_F}{r^6 \tau_F} \int_0^\infty \varepsilon_A(\omega) \overline{F}_D(\omega) \omega^{-4} d\omega \tag{21}$$

The equation (21) now shows the basic physics of the Förster energy transfer. The rate is proportional to the overlap of the normalized donor fluorescence spectrum and the acceptor absorption spectrum, decreases with 6th power of donor-acceptor distance, and depends on the donor fluorescence quantum efficiency and lifetime, and the mutual orientation of the donor and acceptor transition dipole moments. The complete expression for the energy transfer, expressed in the units of wavelength λ, is given by

$$\Gamma_{DA} = \frac{(9000\ln 10)\kappa^2\phi_F}{128\pi^5 n^4 N_A r^6 \tau_F}\int_0^\infty \varepsilon_A(\lambda)\overline{F}_D(\lambda)\lambda^4 d\lambda \qquad (22)$$

where N_A is Avogadro's number, and the refractive index n appears because the interaction between the two dipoles occurs in a dielectric medium rather than in vacuum.

It is now possible to define the *Förster distance* R_0 as a distance between the donor and acceptor at which the energy transfer rate is equal to the fluorescence rate of the donor in the absence of acceptor, i.e. at which $\Gamma_{DA} = 1/\tau_F$. It follows that

$$R_0^6 = \frac{(9000\ln 10)\kappa^2\phi_F}{128\pi^5 n^4 N_A}\int_0^\infty \varepsilon_A(\lambda)\overline{F}_D(\lambda)\lambda^4 d\lambda \qquad (23)$$

For a given pair of donor and acceptor molecules the R_0 is a constant and the rate of energy transfer is simply given by

$$\Gamma_{DA} = \frac{1}{\tau_F}\left(\frac{R_0}{r}\right)^6 \qquad (24)$$

One way to experimentally measure the energy transfer is to measure relative changes in fluorescence spectra of both the donor and acceptor upon excitation of the donor only. In case of zero energy transfer, only the fluorescence spectrum of the donor is observed. In case of 100% energy transfer, only the fluorescence spectrum of the acceptor can be measured. At R_0 the efficiency of the energy transfer is 50% and the energy is equally distributed between donor and acceptor fluorescence. Typically, R_0 is on the order of 2 – 5 nm, which is comparable to the size of many proteins and to the thickness of biological membranes. It is thus possible to measure the efficiency of energy transfer between donor and acceptor labels in biological samples and to deduce from the results the distances between, e.g., binding sites on the proteins. Recently, Förster energy transfer is increasingly being used in the study of biochemical and biophysical processes, such as protein folding, on single molecule level.

Another way to study the energy transfer process is to measure the fluorescence lifetime of the donor in the presence of the acceptor, and compare it with the donor fluorescence lifetime in the absence of the acceptor. With increasing efficiency of the energy transfer the measured lifetime shortens compared to the case of zero energy transfer.

4.3. Dexter energy transfer

In donor-acceptor systems where the dipole-dipole energy transfer mechanism is negligible due to weak absorption or emission transition dipoles the energy can be still transferred via electron-exchange mechanism, first described by D.L. Dexter. Since the mechanism involves exchange of electrons between the donor and acceptor molecules, as schematically shown in Figure 32, it depends on the overlap of the respective molecular orbitals and is effective only on very short D-A distances. The theoretical description begins with the transfer probability expressed by the general Fermi's golden rule.

$$\Gamma_{DA} = \frac{\pi}{2\hbar^2}\left(\left|H_{DA}^{c}\right|^2 + \left|H_{DA}^{e}\right|^2\right)\delta(\omega_D - \omega_A) \qquad (25)$$

The equation (25) is more general than (2) as it contains both the Coulomb $\left|H_{DA}^{c}\right|$ and exchange $\left|H_{DA}^{e}\right|$ interaction terms. In the treatment of the dipole-dipole energy transfer the exchange term could be neglected because at the relevant D-A distances it is much weaker than the Coulomb term. On the other hand, for weak transition dipole moments the Eq. (9) shows that the Coulomb term is very small and the exchange term becomes the dominant interaction.

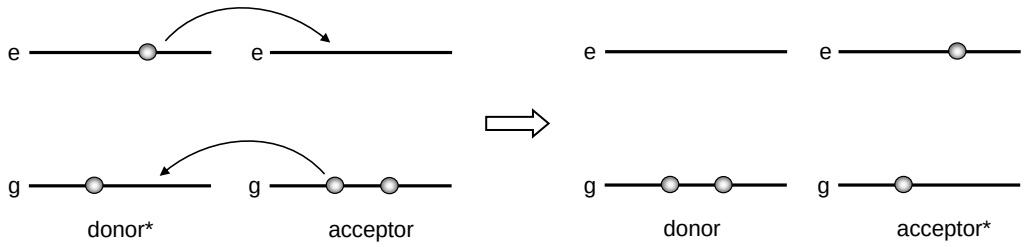

Figure 32

The exchange term can be expressed as

$$\left|H_{DA}^{e}\right| = \int \psi_D(2)\psi_A^{u}(1)(H_{DA}^{e})\psi_D^{u}(1)\psi_A(2)dr \qquad (26)$$

where the indexes 1 and 2 refer to the different electrons originally located on the donor and acceptor molecules. It is now necessary to include the spin state of the electrons by including spin wavefunctions χ as

$$\psi(1) \rightarrow \psi(1)\chi(1) \tag{27}$$

The exchange term now takes the from of

$$\left|H_{DA}^{e}\right| = \int \psi_D(2)\chi_D(2)\psi_A^u(1)\chi_A^u(1)(H_{DA}^{e})\psi_D^u(1)\chi_D^u(1)\psi_A(2)\chi_A(2)drd\sigma \tag{28}$$

Since the Hamiltonian in Eq. (28) does not operate on the spin wavefunctions the integral can be separated as

$$\left|H_{DA}^{e}\right| = \int \psi_D(2)\psi_A^u(1)(H_{DA}^{e})\psi_D^u(1)\psi_A(2)dr \int \chi_D(2)\chi_A^u(1)\chi_D^u(1)\chi_A(2)d\sigma \tag{29}$$

The second integral can be re-written according to the electron coordinates as

$$\int \chi_D(2)\chi_A^u(1)\chi_D^u(1)\chi_A(2)d\sigma = \int \chi_D(2)\chi_A(2)d\sigma_2 \int \chi_A^u(1)\chi_D^u(1)d\sigma_1 \tag{30}$$

As a result of the *orthogonality* of the spin wavefunctions of the same electrons the expression (30) is different from zero only when

$$\chi_D(2) = \chi_A(2) \quad \text{and} \quad \chi_D^u(1) = \chi_A^u(1) \tag{31}$$

The physical meaning of the condition (31) is that energy transfer by the exchange mechanism can occur only when the ground states of the D and A have the same spin, and at the same time the excited states of the D and A are in the same spin states. The condition for the ground states is fulfilled automatically since the ground states are singlets. The energy transfer can thus occur between D and A which have the same spin multiplicity of the excited states, i.e. between singlet D and A, or between triplet D and A. Singlet-singlet transitions are often allowed and the energy transfer between excited singlets is dominated by the dipole-dipole Förster mechanism. The Dexter exchange mechanism is thus often synonymous with triplet-triplet energy transfer. However, care must be taken in cases where S_0-T_1 transitions are partly allowed (efficient phosphorescence) or where S_0-S_1 transitions are forbidden.

The first integral of the Eq. (29) contains the exchange operator

$$H_{DA}^{e} = \frac{e^2}{\kappa r} \tag{32}$$

The use of this operator in the Eqs. (29) and (26) leads to the following rate of energy transfer by electron exchange mechanism

$$\Gamma_{DA}^{e} \propto \frac{2\pi}{\hbar} Z^2 \int_0^{\infty} \bar{\varepsilon}_A(\omega) \bar{F}_D(\omega) d\omega \qquad (33)$$

The integral in the Eq. (33) contains the overlap of normalized donor fluorescence and normalized acceptor absorption spectra. Since at least one of these transitions is usually spin-forbidden, the physical meaning of this integral is to express the condition for the energy difference between the donor and acceptor excited states. The quantity Z^2 is a function of the D-A distance r

$$Z^2 \propto \exp(-2r / L) \qquad (34)$$

where L is an average Bohr radius for the excited and ground state of the donor and acceptor molecules, respectively. Since, according to the dependence (34), the energy transfer rate is an exponentially decreasing function of the D-A distance, energy transfer by the Dexter exchange mechanism occurs efficiently only over very short distances on the order of ~ 1 nm.

4.4. Photoinduced electron transfer

In some aspects, the Dexter exchange mechanism of energy transfer is similar to another light-induced intermolecular process, the electron transfer. Electron transfer is usually treated as a subject of physical chemistry, and here only the main features of the process are summarized. The mechanism is schematically shown in Figure 33.

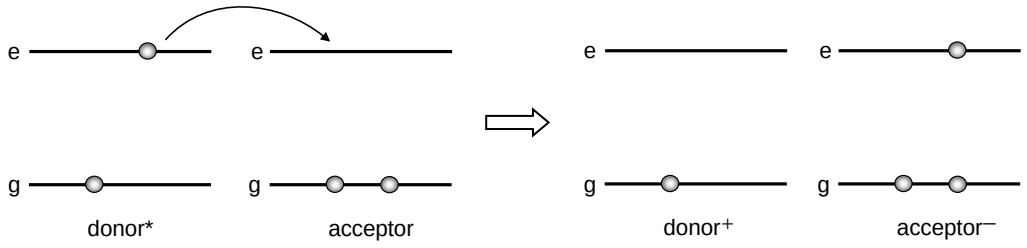

Figure 33

Compared to the Dexter energy transfer, only the excited state electron is transferred from the donor to the acceptor molecule. The result is the creation of the D^+ and A^- ions. As with the energy transfer, the necessary condition for the electron transfer to occur is overlap of the donor and acceptor molecular orbitals. The dependence of the transfer rate constant on the D-A distance can be simplified as

$$\Gamma_{DA}^{el} \propto \exp\left[-\beta(r-L)\right] \tag{35}$$

where L is again the average Bohr radius and the coefficient β is a quantity inversely proportional to the overlap between the donor and acceptor electron orbitals. The Eq. (35) is the expression of the exponential decrease of electron transfer efficiency with increasing intermolecular separation. Besides the distance, other parameters affecting the electron transfer rate are the potential energy functions of the donor and acceptor, mutual orientation, shape and nodal character of the respective electron orbitals, and spin states.

5. External field effects

External electric or magnetic fields acting upon organic molecules can change the energy levels of their ground and excited states. When the changes in the ground and excited states are different the optical transition energies change, leading to splitting and shifts in the spectral lines. Spectral changes caused by external electric field are called Stark effect while those caused by magnetic field are known as Zeeman effect.

5.1. Stark effect

The effects of electric field on the optical properties of molecules can be best illustrated using classical electromagnetic approach. The nature of the effect will vary depending on whether the molecule has a permanent electric dipole moment in at least one of its electronic states.

1. Polar molecules

Let us assume that a molecule has an electric dipole moment $\mathbf{m}_G$ in its ground state and a dipole moment $\mathbf{m}_E$ in its excited state. Energy of an electric dipole **m** in the electric field **F** is generally a dot-product of the two vectors

$$E = -\mathbf{m} \cdot \mathbf{F} \tag{1}$$

The energy levels of the molecular ground and excited states in an electric field F will be accordingly modified as

$$E_G^F = E_G^0 - \mathbf{m}_G \cdot \mathbf{F} \qquad \text{and} \qquad E_E^F = E_E^0 - \mathbf{m}_E \cdot \mathbf{F} \tag{2}$$

The optical transition energy in the electric field is the difference

$$\Delta E^F = E_E^F - E_G^F = \Delta E^0 - \left(\mathbf{m}_E - \mathbf{m}_G\right) \cdot \mathbf{F} \tag{3}$$

where ΔE^0 is the energy of the transition in the absence of the electric field. The Eq. (3) shows that the transition energy in the presence of the electric field is shifted by an amount which is proportional to the *difference* $\Delta\mathbf{m}$ of the permanent dipole moments in the molecular ground and excited states. Spectrally, the absorption or fluorescence peak is shifts proportionally to the first power of **F**, and the phenomenon is accordingly called *linear Stark effect*. Whether the shift is to the blue or red, i.e. to higher or lower

energies, depends, as obvious from the Eq. (3), on the relative magnitudes of $\mathbf{m}_G$ and $\mathbf{m}_E$. Molecules with stronger dipole moment in their excited states will experience red spectral shift.

2. Non-polar molecules

For molecules without permanent dipole moments the linear Stark effect is zero. In such molecules, the external electric field produces an induced dipole moment proportional to the polarizability α

$$\mathbf{m}^{ind} = -\alpha\mathbf{F} \tag{4}$$

The energy of the induced dipole moment in the electric field **F** is then according to (1)

$$E = \alpha F^2 \tag{5}$$

The optical transition energy will again be modified as

$$\Delta E^F = E_E^F - E_G^F = \Delta E^0 - \Delta\alpha F^2 \tag{6}$$

where $\Delta\alpha$ is now the *difference* between the polarizabilities of the ground and excited states. The spectrum is shifted by an amount which is proportional to the second power of the electric field intensity and the corresponding phenomenon is called *quadratic Stark effect*. The direction of the spectral shift again depends on the sign of $\Delta\alpha$ and can be either blue or red.

The above discussion is based on considering the effect of electric field on *one molecule*. In practical experiments on organic molecules in condensed phase there are large numbers of molecules oriented randomly with respect to the field **F**. Moreover, local dielectric constant inhomogeneities around the molecule and symmetry of the molecular environment will almost invariably induce a permanent dipole moment in non-polar molecules even in the absence of the external electric field. The common observation is thus of broadening and splitting of the optical spectra rather than pure shift. The effect most often observed is linear Stark shift with small contribution of the quadratic part. Purely quadratic Stark effect has been observed only recently using single aromatic molecules in organic crystals at low temperatures.

The Stark effect has an important application in the experimental technique of electroabsorption where the difference in absorption spectra with and without the presence of the electric field is measured. The form of the difference spectrum as either first or second derivative of the original absorption spectrum allows, e.g., to distinguish

Frenkel exciton from charge-transfer states.

5.2. Zeeman effect

Similar to the Stark effect, the Zeeman effect describes the influence of external magnetic field on the molecular optical properties. The main difference is that each electron involved in the optical transition possesses a magnetic dipole moment in the form of the orbital moment and spin moment. In many cases, the contribution from the spin moment is negligible and the phenomena observed can be explained based on the orbital magnetic moment only (normal Zeeman effect).

Generally, the energy of a magnetic dipole moment $\boldsymbol{\mu}$ in external magnetic field **B** is given by

$$E = -\boldsymbol{\mu} \cdot \mathbf{B} \tag{7}$$

The magnetic dipole moment of an electron associated with its orbital angular momentum L is expressed as

$$\boldsymbol{\mu}_{orbital} = \frac{-e}{2m_e}\mathbf{L} \tag{8}$$

For a magnetic field pointing in the z-direction we may take the z-component L_z of **L** to write

$$E = \frac{e}{2m} L_z B = m_l \mu_B B \tag{9}$$

where we made use of the definition of Bohr magneton μ_B

$$\mu_B = \frac{e\hbar}{2m_e} \tag{10}$$

and the relationship between L_z and the orbital magnetic quantum number m_l

$$L_z = m_l \hbar \tag{11}$$

The equation (9) gives an expression for energy levels spaced equally due to the quantum number m_l. The displacement of these energy levels from the zero-field value gives the observed multiplet splitting of spectral lines in Zeeman effect.

In cases where electron spin contributes to the observed Zeeman effect the

equation (9) must be replaced with a more general relation

$$E = \frac{e}{2m}(\mathbf{L} + 2\mathbf{S}) \cdot \mathbf{B} = g_L \mu_B m_j B \qquad (12)$$

where g_L is a geometrical factor (Lande's factor) accounting for the different orientations of the orbital and spin moments, and m_j is the total magnetic moment quantum number. Historically, the effect of magnetic field with the contribution of electron spins has been called anomalous Zeeman effect.

6. Principles of high resolution optical spectroscopy

Conventional absorption and fluorescence spectra provide only limited information on the electronic and vibrational structure of molecular states. Usually, it is possible to assign the observed absorption bands to individual singlet states S_1, S_2 and higher, and to obtain Franck-Condon factors for limited vibronic transitions. To reveal the wealth of information contained in the optical spectra it is necessary to remove the various types of broadening of the absorption or fluorescence bands. This Chapter introduces principles of several spectroscopic methods that enable study of the detailed structure of vibronic transitions of complex molecules.

6.1. Homogeneous and inhomogeneous spectral broadening

In Chapter 2 it was shown that the shape of an absorption spectral line corresponding to the transition between two quantum energy levels has a Lorentzian profile, and that commonly observed absorption spectra of aromatic molecules in solutions are envelopes of a large number of Lorentzian lines originating from different vibronic transitions. In usual absorption measurements samples with concentrations on the order of 10^{-5} M or higher are used, which means that 10^{15} - 10^{20} molecules are probed at the same time. From this point, it is interesting to look at the effect of ensemble averaging of optical spectra. Figure 34 shows a fluorescence spectrum at room temperature of carbocyanine molecules adsorbed on a glass surface at ensemble concentrations (left) and a corresponding fluorescence spectrum measured from a single molecule (right). The comparison shows that the spectra are identical which is an example of *homogeneous broadening* of optical spectra.

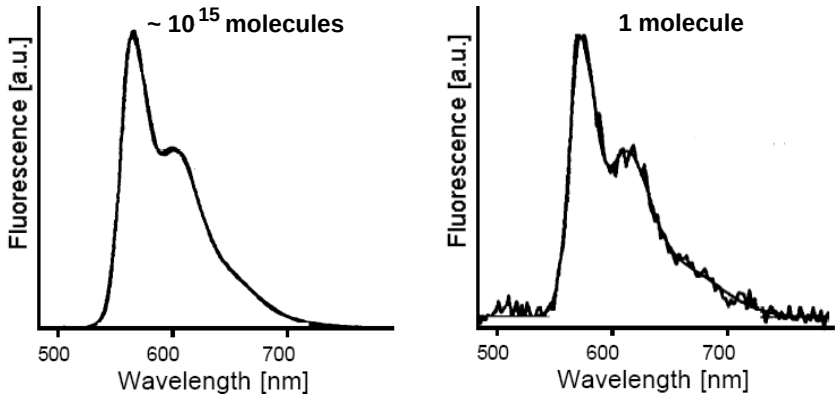

Figure 34 (reprinted from K. Weston et al, J. Chem. Phys. 109 (1998) 7474)

In addition to the multitude of vibronic transitions active at room temperature, Doppler or collisional broadening in the case of gases or solutions, or interaction with matrix phonons in the case of molecules doped into solid matrices are the main contributions to the observed homogeneous spectrum at room temperature. Thus, to decrease the homogeneous linewidth, it is necessary to decrease the number of active phonon or vibronic modes. This can be done by lowering the temperature of the experiment down to the temperature of liquid helium, i.e. to 4.2 K or below. The effect of lowering the temperature on the ensemble absorption spectra of pseudoisocyanine molecules is

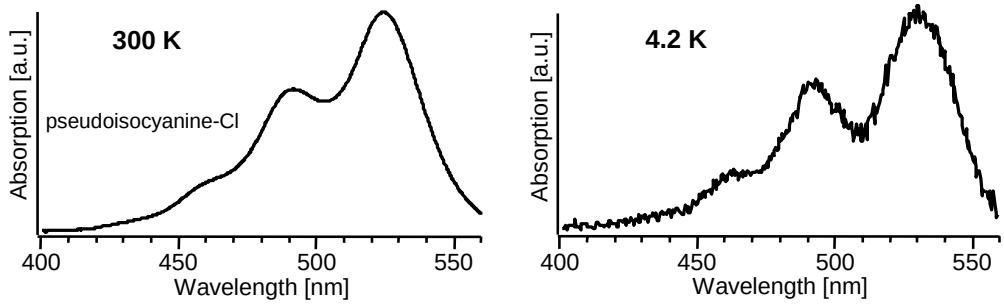

Figure 35

shown in Figure 35. At the temperature of 4.2 K all optical transitions are essentially represented by zero-phonon lines; still the absorption spectra at 300 K and 4.2 K are almost identical. This is a result of *inhomogeneous broadening* present at the cryogenic temperatures. The origin of inhomogeneous broadening is shown schematically in Figure 36. In the solid matrix, each molecule is located in slightly different local environment.

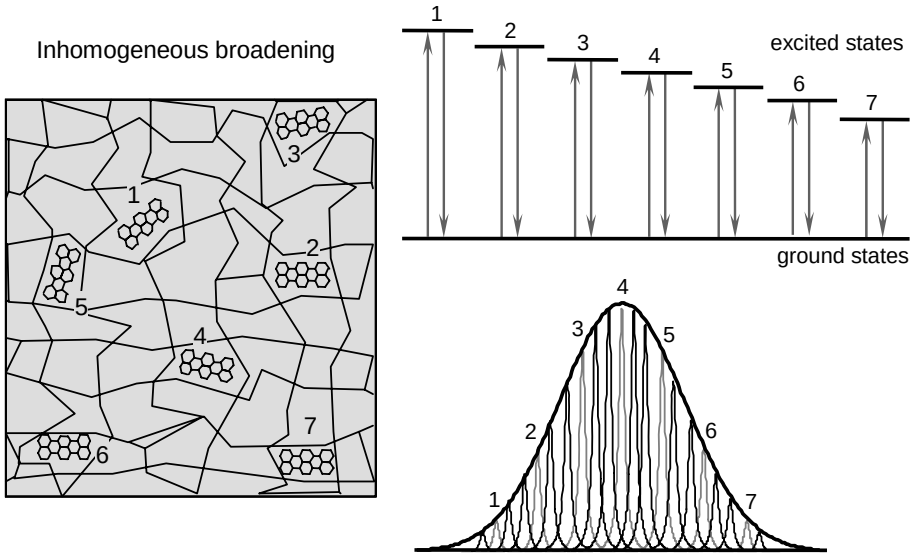

Figure 36

Mechanical strain and electrostatic interactions modify differently the electronic energy levels of molecules at each location and cause each molecule to have slightly different optical transition energy. Even though the optical transitions themselves now appear as narrow Lorentzian lines, the overall spectrum is an envelope of spectral lines of a large number of molecules, as shown in Fig. 36.

The inhomogeneous broadening can be partly or completely removed using special spectroscopic techniques. Those most often used will be introduced in the following sections.

6.2. Fluorescence line-narrowing

The method of fluorescence line-narrowing is based on the excitation of fluorescence spectra at low temperatures with spectrally narrow laser light. The laser selectively excites only those molecules in the inhomogeneous manifold whose optical transition is in resonance with the laser frequency. The result is the appearance of a series of sharp fluorescence lines corresponding to the vibronic transitions $S_1(v'=0) \rightarrow S_0(v \geq 1)$. An example of the effect of excitation light on the structure of fluorescence spectra is shown in Figure 37 for the molecules of a bisanthene derivative at 4.2 K. Excitation with a broadband conventional source leads to the usual broad fluorescence bands. Excitation with laser light tuned to the peak of the lowest energy absorption band is accompanied by the appearance of a series of sharp lines both in the main band and in the first vibrational band. The intensity of the lines is determined by the respective Franck-Condon factors. Even though the lines are narrow, the fluorescence line-narrowing does not enable the determination of the true homogeneous line due to residual inhomogeneous broadening, matrix dynamics and power broadening.

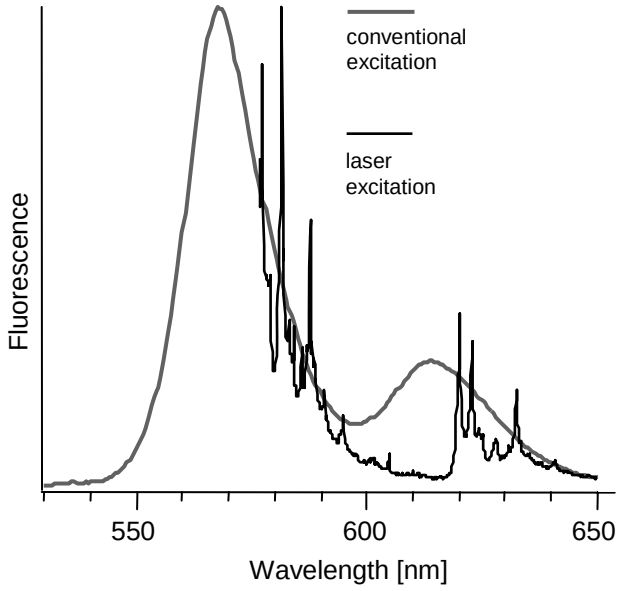

Figure 37

6.3. Spectral hole-burning

The technique of spectral hole-burning is in many respects similar to the method of fluorescence line-narrowing. The sample is again irradiated with spectrally narrow laser light tuned within the inhomogeneous profile. Only molecules with their optical transition in resonance with the laser frequency will absorb the light. In contrast to the previous method, however, the excitation light is very strong and leads to a permanent change to the absorbing molecules. The change can be photochemical of photophysical (non-photochemical) in nature and the phenomena are accordingly called photochemical (PHB) and non-photochemical hole-burning (NPHB). The light-induced change leaves the number of molecules absorbing at particular frequency altered and the corresponding spectrum shows a dip, or "hole" at the frequency. An example of spectral hole in the absorption spectra of J-aggregates of pseudoisocyanine molecules is shown in Figure 38.

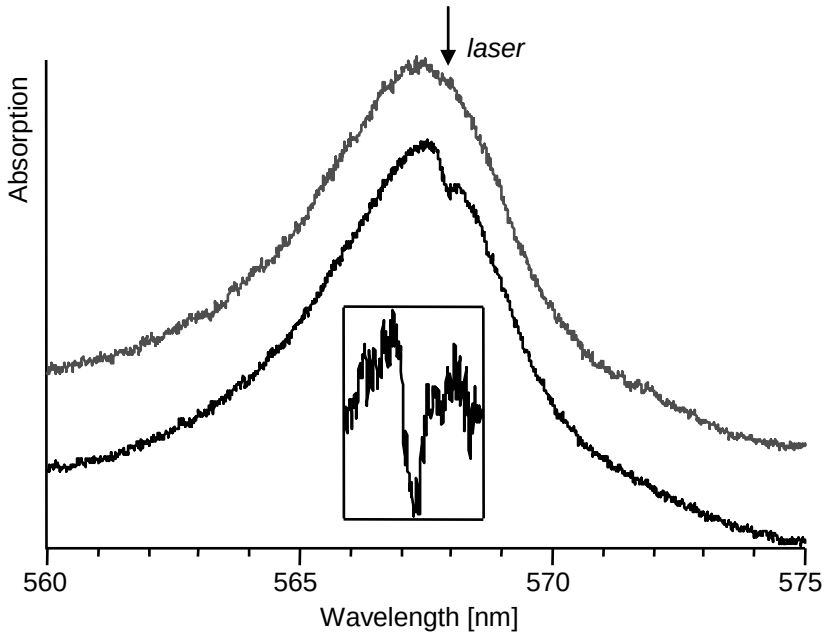

Figure 38

The profile of the spectral hole, when measured carefully, is a mirror image of the absorption lineshape and provides information on the homogeneous width of the spectral line at low temperatures. The linewidth can be expressed as

$$\gamma / 2 = \frac{1}{2\pi T_1} + \frac{1}{\pi T_2^*} \qquad (1)$$

where T_1 is the excited state depopulation time (fluorescence lifetime) and T_2^* is phase relaxation time (pure dephasing time) describing phase relationship of the excited-state wavefunctions. Measuring the spectral hole profile and its development in time thus

provides a tool to study various excited state relaxation processes, as well as relaxation processes occurring in the solid matrix.

6.4. Single molecule spectroscopy at cryogenic temperatures

The inhomogeneous broadening can be most obviously removed by measuring spectra of individual molecules. The large width of the inhomogeneous band now provides an advantage as it is not necessary to reduce the actual number of molecules in the measured volume to 1. Figure 39 illustrates the effect of decreasing concentration of molecules in the sample on the optical spectra. The numerical simulation in the left part of the figure shows that single-molecule lines start appearing

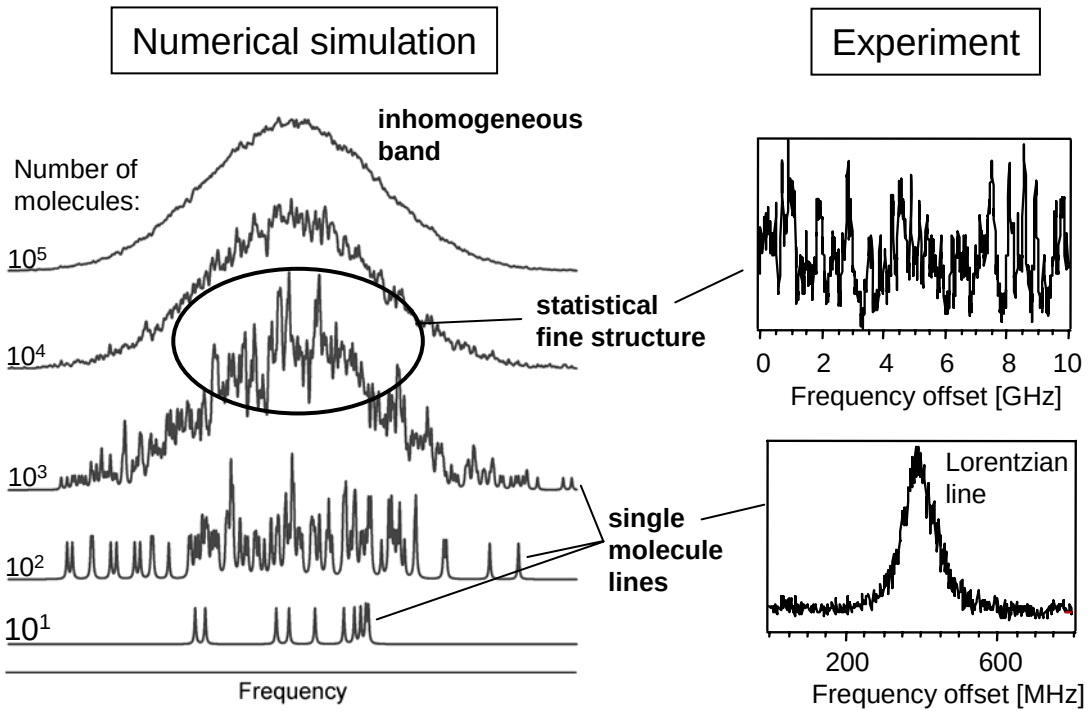

Figure 39

at the wings of the inhomogeneous band even when there are thousands of molecules present in the excited volume. The experimental results in the right part of the figure correspond nicely with the numerical predictions. The single-molecule absorption (excitation) spectral line at cryogenic temperature has a Lorentzian profile as predicted by theory, with a width close to the radiative lifetime. Compared to the previous spectroscopic methods which are based on spectral selection of large numbers of molecules with the same transition energy due to accidental degeneracy and which

provide information on the *average values* of physical observables, single-molecule spectroscopy provides qualitatively different information based on parallel measurements on large numbers of individual molecules, resulting in *distributions of actual values of physical observables*.

6.5. Single-molecule detection at room temperature

Though strictly speaking not a high-resolution spectroscopic technique, single-molecule detection at room temperature retains the advantage of removing ensemble averaging from the measured phenomena. At room temperature, however, the spectral selectivity due to the inhomogeneous broadening is no longer applicable and individual molecules for experiments must be isolated spatially within extremely diluted microscopic samples. Also, the requirements for high absorption cross-section, high fluorescence quantum efficiency and high photostability are much stricter at room temperature.

Literature:

[1] R. Loudon: *The Quantum Theory of Light.* Oxford University Press (3rd edition), Oxford, 2000

[2] G.M. Barrow: *Introduction to Molecular Spectroscopy.* McGraw-Hill, New York, 1962

[3] D.K. Ferry: *Quantum Mechanics.* Institute of Physics Publishing (2nd edition), Bristol, 2001

[4] F. Mandel: *Quantum Mechanics.* John Wiley & Sons Ltd, Chichester, 1992

[5] J.B. Birks: *Photophysics of Aromatic Molecules*. Wiley-Interscience, London, 1970

[6] P.W. Atkins: *Physical Chemistry.* Oxford University Press (6th edition), Oxford, 1998

[7] J.R. Lakowicz: *Principles of Fluorescence Spectroscopy*. Plenum Press, New York, 1983

[8] W. Demtroeder: *Molecular Physics*. Wiley-VCH, Weinhem, 2005.

[9] A.S. Davydov: *Theory of Molecular Excitons*. Plenum Press, New York, 1971

[10] M. Kasha, in: *Spectroscopy of the Excited State*. Plenum Press, New York, 1976 (pp. 337-363)

[11] M. Kasha et al, *Pure and Applied Chemistry* 11 (1965) 371-392

[12] F. Brouwer, in: *Conformational Analysis of Molecules in Excited States*. Wiley-VCH, New York, 2000. (pp.177-236)

[13] *Resonance Energy Transfer* (D.L. Andrews amd A.A. Demidov, Eds.). John Wiley & Sons Ltd, Chichester, 1999

[14] D.L. Dexter, *J. Chem. Phys.* 21 (1953) 836

[15] G.J. Kavarnos: *Fundamentals of Photoinduced Electron Transfer.* Wiley-VCH, New York, 1993.